

[Electronic Supplementary Information]

# Risk-based Uncertainty Assessment to Identify Key Sustainability Hurdles for Emerging CO<sub>2</sub> Utilization Technologies

Jeehwan S. Lee<sup>a</sup>, Juyeong Jung<sup>a</sup>, Kosan Roh<sup>b</sup>, Seongmin Heo<sup>c</sup>, Ung Lee<sup>d</sup>, Jay H. Lee<sup>a\*</sup>

<sup>a</sup> Department of Chemical and Biomolecular Engineering, Korea Advanced Institute of Science and Technology (KAIST), 291 Daehak-ro, Yuseong-gu, Daejeon 34141, Republic of Korea

<sup>b</sup> Department of Chemical Engineering and Applied Chemistry, Chungnam National University, Daejeon 34141, Republic of Korea

<sup>c</sup> Department of Chemical Engineering, Dankook University, Yongin 16890, Republic of Korea

<sup>d</sup> Clean Energy Research Center, Korea Institute of Science and Technology (KIST), Seoul 02792, Republic of Korea

\*Corresponding Author: [jayhlee@kaist.ac.kr](mailto:jayhlee@kaist.ac.kr)

## 1. Nomenclature

### *Uncertainty Classification*

$y^r$	Performance indicator for sustainability aspect $r$
$y_i^r$	Performance indicator for aspect $r$ evaluated at the $i$ -th Monte Carlo instance
$S^r$	Target criteria value for sustainability aspect $r$
$L_c$	Label corresponding to class $c$ where $c = s, f$
$L_s$	Classification label for successfully meeting target criteria
$L_f$	Classification label for failing to meet target criteria
$x_j$	Value of uncertain input $j$
$X$	Vector of uncertain inputs
$Y^r$	Class outcome for indicator $y^r$
$R$	Number of sustainability criteria for uncertainty classification
$N$	Number of Monte Carlo simulations for uncertainty propagation
$J$	Number of uncertain inputs

$M_{N \times J}^0$	A $N \times J$ matrix of Monte Carlo sampled parameter values
$M_{N \times J}^S$	A $N \times J$ matrix of categorized parameter values corresponding to “success” kernel
$M_{N \times J}^F$	A $N \times J$ matrix of categorized parameter values corresponding to “failure” kernel
$V_{c_j}$	Column vector of parameter matrix $M_c$ where $c = s, f$ corresponding to index of input $j$
$W_c$	Number of non-zero column elements in $V_{c_j}$
$h_{c_j}$	Distribution bandwidth determined by Silverman’s rule for the kernel vector $V_{c_j}$

### *Risk Quantification*

$RS_j$	Risk score of uncertain input $j$
$D$	Final sustainability decision for multi-criteria scenario

### *Performance Indicator Calculation*

$uCOGM$	Index representing unit cost of goods manufactured indicator (USD/ton of functional unit)
$CF$	Index representing specific carbon footprint indicator (ton-CO <sub>2</sub> eq./ton of functional unit)
$f^{IEC}$	Lang factor for equipment installation
$f^{DCC}$	Lang factor for direct capital costs from installed equipment cost
$f^{ICC}$	Lang factor for indirect capital costs from installed equipment cost
$f^{WC}$	Lang factor for working capital from fixed capital expenses
$f^{MNT}$	Lang factor for maintenance costs (fixed OPEX)
$f^{ADM}$	Lang factor for administration costs (fixed OPEX)
$f^{OH}$	Lang factor for plant overhead costs (fixed OPEX)
$f^{LB}$	Lang factor for laboratory costs (fixed OPEX)
$LT$	Plant lifetime in years
$d$	Plant capital discount factor (interest rate)

### *Component Abbreviations*

$TREA$	Triethylamine, N(CH <sub>2</sub> CH <sub>3</sub> ) <sub>3</sub>
$nBIM$	<i>n</i> -butyl imidazole, C <sub>7</sub> H <sub>12</sub> N <sub>2</sub>

## **2. Risk assessment and naïve Bayesian classification**

The naïve Bayesian classifier is a probabilistic classifier that is derived from the *maximum a posteriori* (MAP) expression:

$$f(X) = \operatorname{argmax}_{L_c} P(Y = L_c|X), \quad c = s, f \quad (\text{S1})$$

Applying Bayes rule to eqn. (1) gives us the following:

$$f(X) = \operatorname{argmax}_{L_c} \frac{P(X|Y = L_c)P(Y = L_c)}{P(X)} \quad (\text{S2})$$

where  $X = (x_1, x_2, \dots, x_j, \dots, x_J)$  is the set of feature values, or in the context of this work, the set of sampled uncertain input values (Step 3). The denominator term  $P(X)$  functions as a normalizing constant and is equal regardless of the class outcome so it is subsequently ignored.

$$f(X) = \operatorname{argmax}_{L_c} P(X|Y = L_c)P(Y = L_c) \quad (\text{S3})$$

The goal of Bayesian classifiers is to construct the posterior distribution  $P(X|Y = L_c)$  for each class  $L_c$ . If the values of uncertainties  $x_j$  are not discrete, and/or without a sufficiently large training set, computing the joint distributions for every possible realization of  $X$  is computationally intractable. Consequently the conditional independence assumption is applied, in which case eqn. S3 becomes:

$$\hat{f}(X) = \operatorname{argmax}_{L_c} P(Y = L_c) \prod_{j=1}^J P(x_j | L_c) \quad (\text{S4})$$

Applying the naïve assumption reduces the number of posteriors to  $2^J$  where the probabilities  $P(x_j | L_c)$  are derived from each input's class likelihood functions. This serves as the classical derivation for the naïve Bayes classifier. The Monte Carlo simulations essentially function as a generator of training data. Using the constructed class likelihoods, the classifier  $\hat{f}(X)$  outputs the class  $L_c$  with the highest probability when a new set of input feature values are observed.

Many studies have focused on the prediction accuracy of  $\hat{f}(X)$  and the robustness of the naïve assumption.<sup>1</sup> In the decision network (Figure 6) the uncertainties have edges directed to the indicators,

which implies conditional dependence between the inputs. For this we provide two justifications: first, the NBC has demonstrated to be robust even in domains that involve significant conditional dependencies.<sup>2-4</sup> Second and more importantly, in the quantification of sustainability risk we primarily concern ourselves with the class likelihood functions by computing the area of the difference and observing points of intersection. Conditional dependence becomes more relevant in the accurate predictions of the sustainability outcomes of future scenarios. If highly dependent uncertainties can be known *a priori*, techniques such as clustering can be employed to group multiple inputs into a single feature  $x_j$ .

### **3. Methodology application to the Carbon-to-X formic acid process**

#### **3.1. Code availability**

The MATLAB code for sustainability risk assessment of the CtX formic acid process is available online in the following Github repository:

*[https://github.com/KAIST-LENSE/SusRisk\\_CDU](https://github.com/KAIST-LENSE/SusRisk_CDU)*

#### **3.2. Detailed process specifications**

The SMR process for conventional hydrogen generation and the CtX formic acid process were both simulated in AspenPlus™ v10. The process flowsheets and mass balance tables are shown in Figures S1, S2 and Tables S1, S2 respectively.

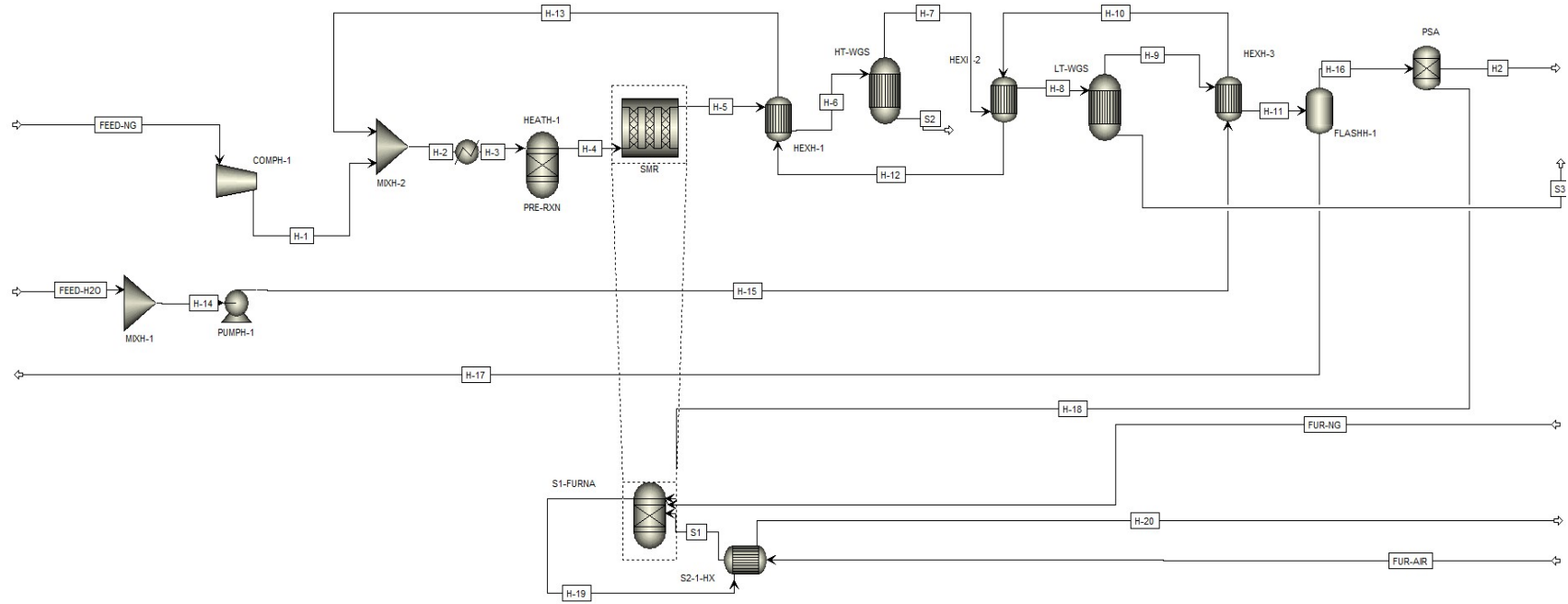


**Figure S1** Process flow diagram of the steam methane reforming (SMR) process for hydrogen generation, simulated with AspenPlus™ v10.

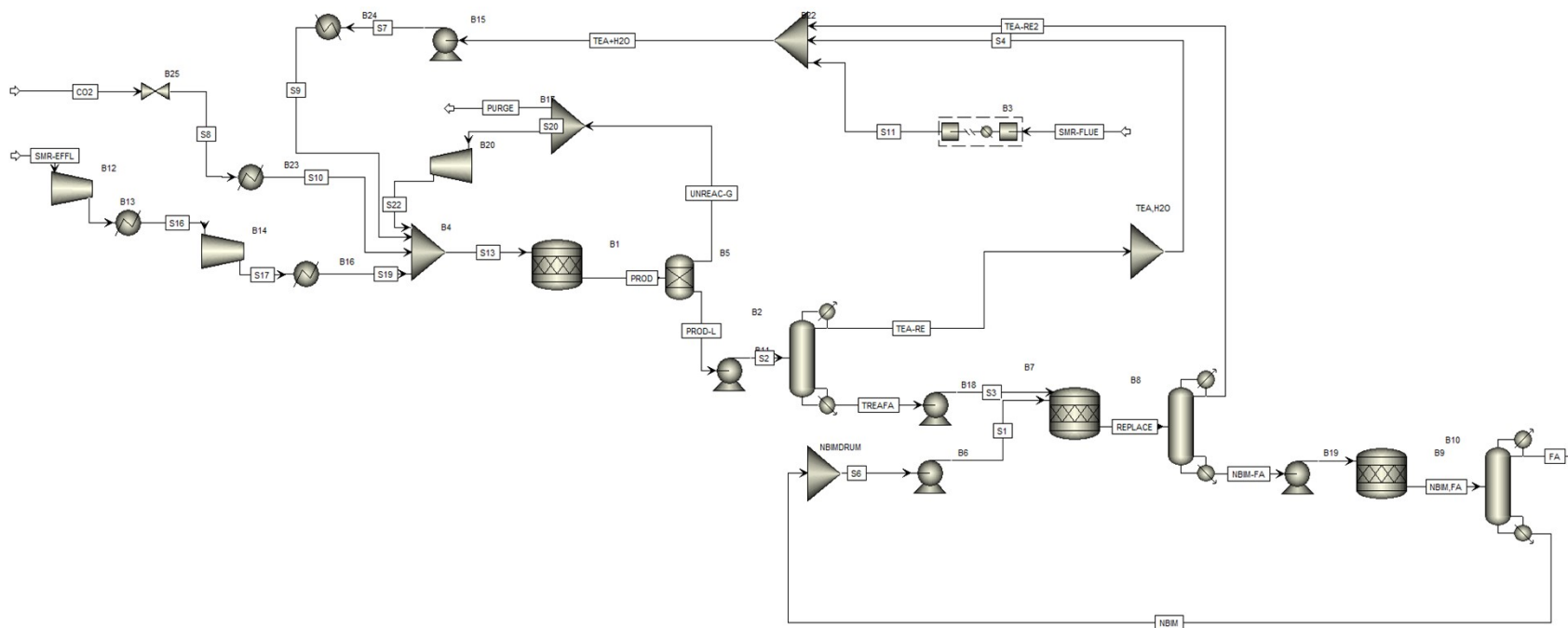


**Figure S2.** Process flow diagram of the CtX formic acid process, simulated with AspenPlus™ v10.

**Table S1.** Mass and energy balance table of the SMR process for hydrogen generation.

Units		FEED-H2O	FEED-NG	FUR-AIR	FUR-NG	H2	H-1	H-2	H-3	H-4	H-5
Phase		Liquid	Vapor	Vapor	Vapor	Vapor	Vapor	Vapor	Vapor	Vapor	Vapor
C		25	25	25	25	40	80.91	298.80	500	434.64	950
bar		1	20	1.3	20	22.5	35	35	35	35	29
Molar Enthalpy	kcal/mol	-69.04	-17.90	0.00	-17.90	0.11	-17.42	-45.52	-43.38	-41.94	-17.49
Mass Enthalpy	kcal/kg	-3832.11	-1101.00	-0.07	-1101.00	54.46	-1071.73	-2590.15	-2468.82	-2468.82	-1465.51
Enthalpy Flow	Gcal/hr	-4.32	-0.38	0.00	-0.10	0.01	-0.37	-3.80	-3.62	-3.62	-2.15
Mole Flow	kmol/hr	62.51	21.04	97.50	5.65	70.55	21.04	83.55	83.55	86.41	123.01
Mass Flow	kg/hr	1126.09	342.00	2824.50	91.77	142.22	342.00	1468.10	1468.10	1468.10	1468.10
<b>Mole Fractions</b>											
CH4		0	0.986	0	0.986	0	0.986	0.248	0.248	0.230	0.013
CO2		0	0	0	0	0	0	0	0	0.016	0.044
H2O		1	0	0	0	0	0	0.748	0.748	0.690	0.304
H2		0	0	0	0	1	0	0	0	0.063	0.523
CO		0	0	0	0	0	0	0	0	0.000	0.117
METHANOL		0	0	0	0	0	0	0	0	5.26E-09	3.70E-09
O2		0	0	0.21	0	0	0	0	0	4.94E-31	3.47E-31
N2		0	0.001	0.78	0.001	0	0.001	2.52E-04	2.52E-04	2.43E-04	1.71E-04
AR		0	0	0.01	0	0	0	0	0	0	0
ETHANE		0	0.0118	0	0.0118	0	0.0118	0.00297139	0.00297139	4.23E-06	2.98E-06
PROPANE		0	0.001	0	0.001	0	0.001	0.00025181	0.00025181	5.12E-10	3.59E-10
ISOBU-01		0	0.0001	0	0.0001	0	0.0001	2.52E-05	2.52E-05	4.58E-14	3.22E-14
N-BUT-01		0	0.0001	0	0.0001	0	0.0001	2.52E-05	2.52E-05	5.88E-14	4.13E-14

**Table S1.** Mass and energy balance table of the SMR process for hydrogen generation. (continued)

Units		H-6	H-7	H-8	H-9	H-10	H-11	H-12	H-13	H-14	H-15
Phase		Vapor	Vapor	Vapor	Vapor	Liquid	Liquid	Liquid	Vapor	Liquid	Liquid
C		310	320	250	190	140	131.11	190.40	386.65	25	26.66
bar		29	23	23	22.5	35	22.5	35	35	1	35
Molar Enthalpy	kcal/mol	-22.84	-23.70	-24.26	-24.86	-66.61	-26.07	-65.50	-54.97	-69.04	-68.99
Mass Enthalpy	kcal/kg	-1913.99	-1985.63	-2032.88	-2083.18	-3697.61	-2184.23	-3636.01	-3051.31	-3832.11	-3829.35
Enthalpy Flow	Gcal/hr	-2.81	-2.92	-2.98	-3.06	-4.16	-3.21	-4.09	-3.44	-4.32	-4.31
Mole Flow	kmol/hr	123.01	123.01	123.01	123.01	62.51	123.01	62.51	62.51	62.51	62.51
Mass Flow	kg/hr	1468.10	1468.10	1468.10	1468.10	1126.09	1468.10	1126.09	1126.09	1126.09	1126.09
<b>Mole Fractions</b>											
CH4		0.013	0.013	0.013	0.013	0	0.013	0	0	0	0
CO2		0.044	0.146	0.146	0.159	0	0.159	0	0	0	0
H2O		0.304	0.202	0.202	0.189	1	0.189	1	1	1	1
H2		0.523	0.624	0.624	0.637	0	0.637	0	0	0	0
CO		0.117	0.015	0.015	0.002	0	0.002	0	0	0	0
METHANOL		3.70E-09	3.70E-09	3.70E-09	3.70E-09	0	3.70E-09	0	0	0	0
O2		3.47E-31	3.47E-31	3.47E-31	3.47E-31	0	3.47E-31	0	0	0	0
N2		1.71E-04	1.71E-04	1.71E-04	1.71E-04	0	1.71E-04	0	0	0	0
AR		0	0	0	0	0	0	0	0	0	0
ETHANE		2.98E-06	2.98E-06	2.98E-06	2.98E-06	0	2.98E-06	0	0	0	0
PROPANE		3.59E-10	3.59E-10	3.59E-10	3.59E-10	0	3.59E-10	0	0	0	0
ISOBU-01		3.22E-14	3.22E-14	3.22E-14	3.22E-14	0	3.22E-14	0	0	0	0
N-BUT-01		4.13E-14	4.13E-14	4.13E-14	4.13E-14	0	4.13E-14	0	0	0	0

**Table S1.** Mass and energy balance table of the SMR process for hydrogen generation. (continued)

Units		H-16	H-17	H-18	H-19	H-20	S1
Phase		Vapor	Liquid	Liquid	Vapor	Vapor	Vapor
C		40	40	40	950	404.23	900
bar		22.5	22.5	22.5	1.3	1.3	1.3
Molar Enthalpy	kcal/mol	-18.73	-68.72	-63.98	-21.92	-26.89	6.56
Mass Enthalpy	kcal/kg	-1777.45	-3813.85	-2067.38	-736.44	-903.51	226.34
Enthalpy Flow	Gcal/hr	-1.87	-1.58	-1.88	-2.82	-3.46	0.64
Mole Flow	kmol/hr	100.00	23.01	29.45	128.60	128.60	97.50
Mass Flow	kg/hr	1053.56	414.53	911.34	3827.61	3827.61	2824.50
<b>Mole Fractions</b>							
CH4		0.016	3.34E-07	0.054	2.04E-33	2.04E-33	0
CO2		0.195	1.00E-04	0.662	0.210	0.210	0
H2O		2.72E-03	1.000	0.009	0.176	0.176	0
H2		0.784	2.83E-06	0.266	2.61E-08	2.61E-08	0
CO		2.31E-03	4.41E-09	0.008	4.53E-08	4.53E-08	0
METHANOL		9.59E-10	1.56E-08	3.26E-09	1.54E-31	1.54E-31	0
O2		0	0	0	0.014	0.014	0.21
N2		2.10E-04	4.95E-10	7.14E-04	0.592	0.592	0.78
AR		0	0	0	7.58E-03	7.58E-03	0.01
ETHANE		3.66E-06	9.05E-11	1.24E-05	1.47E-61	1.47E-61	0
PROPANE		4.42E-10	1.55E-15	1.50E-09	3.48E-89	3.48E-89	0
ISOBU-01		3.96E-14	6.43E-21	1.35E-13	3.41E-117	3.41E-117	0
N-BUT-01		5.08E-14	2.26E-20	1.73E-13	8.19E-117	8.19E-117	0

**Table S2.** Mass and energy balance table of the CtX formic acid process.

<b>Units</b>		<b>CO2</b>	<b>FA</b>	<b>H2O</b>	<b>NBIM</b>	<b>NBIM,FA</b>	<b>NBIM-FA</b>	<b>NBIM-RE</b>	<b>PROD</b>	<b>PROD-L</b>	<b>REPLACE</b>
Phase		Liquid	Liquid	Liquid	Liquid	Liquid	Liquid	Liquid		Liquid	
C		25	53.61	25	25	70	356.09	166.10	120	120	250
bar		150	0.20	1	0.07	0.20	0.33	0.20	100	100	0.33
Molar Enthalpy	kcal/mol	-95.24	-95.06	-68.26	-3.99	-49.04	38.22	4.66	-64.86	-70.64	8.04
Mass Enthalpy	kcal/kg	-2164.17	-2065.22	3789.13	-32.10	-576.30	224.53	37.55	-2228.45	-2280.90	59.23
Enthalpy Flow	Gcal/hr	-7.47	-7.37	-2.39	-0.31	-7.61	2.97	0.36	-80.81	-67.43	1.25
Mole Flow	kmol/hr	78.38	77.56	34.95	77.60	155.19	77.60	77.63	1245.82	954.55	155.19
Mass Flow	kg/hr	3449.51	3569.73	629.65	9635.97	13207.27	13207.72	9637.54	36261.05	29561.08	21060.02
<b>Mole Fractions</b>											
CO2		1	0	0	0	0	0	0	0.1168	0	0
H2		0	0	0	0	0	0	0	0.1170	0	0
O2		0	0	0	0	0	0	0	0	0	0
N2		0	0	0	0	0	0	0	0	0	0
CH4		0	0	0	0	0	0	0	0	0	0
TREA		0	2.70E-05	0	0	1.35E-05	2.70E-05	1.74E-09	0.0216	0.0282	0.5
H2O		0	1.35E-12	1	0	6.75E-13	1.35E-12	2.67E-16	0.6817	0.8897	0
HCOOH		0	1.0000	0	0	0.5000	0	0.0005	0	0	0
NBIM		0	4.52E-12	0	1	0.5000	0	0.9995	0	0	0
TREA-FA		0	0	0	0	0	0	0	0.0629	0.0821	0
NBIM-FA		0	0	0	0	0	1.0000	0	0	0	0.5
CO		0	0	0	0	0	0	0	0	0	0

**Table S2.** Mass and enegy balance table of the CtX formic acid process. (continued)

Units		S1	S2	S3	S4	S5	S6	S7	S8	S15	S17
Phase		Liquid	Liquid	Liquid	Liquid	Liquid	Liquid	Liquid	Liquid	Vapor	Vapor
C		25.01	119.16	307.32	37.68	356.07	25.00	30.56	25.00	151.51	238.82
bar		0.20	0.33	0.20	0.33	0.07	0.07	100	100	50	100
Molar Enthalpy	kcal/mol	-3.99	-70.69	-109.21	-67.39	38.22	-3.99	-64.68	-95.24	0.88	1.49
Mass Enthalpy	kcal/kg	-32.09	-2282.46	-741.84	-3258.13	224.52	-32.10	-2378.93	-2164.17	435.68	738.71
Enthalpy Flow	Gcal/hr	-0.31	-67.47	-8.47	-59.09	2.97	-0.31	-61.74	-7.47	0.07	0.12
Mole Flow	kmol/hr	77.60	954.55	77.60	876.95	77.60	77.60	954.55	78.38	78.39	78.39
Mass Flow	kg/hr	9635.97	29561.08	11423.61	18137.47	13207.72	9635.97	25953.56	3449.51	158.02	158.02
<b>Mole Fractions</b>											
CO2		0	0	0	0	0	0	0	1	0	0
H2		0	0	0	0	0	0	0	0	1	1
O2		0	0	0	0	0	0	0	0	0	0
N2		0	0	0	0	0	0	0	0	0	0
CH4		0	0	0	0	0	0	0	0	0	0
TREA		0	0.0282	0.0000	0.0307	2.70E-05	0	0.1103	0	0	0
H2O		0	0.8897	0.0000	0.9684	1.35E-12	0	0.8897	0	0	0
HCOOH		0	0	0	0	0	0	0	0	0	0
NBIM		1	0	0	0	0	1	0	0	0	0
TREA-FA		0	0.0821	1.0000	0.0009	0	0	0	0	0	0
NBIM-FA		0	0	0	0	1.0000	0	0	0	0	0
CO		0	0	0	0	0	0	0	0	0	0

**Table S2.** Mass and energy balance table of the CtX formic acid process. (continued)

Units		S19	S20	S22	SMR-EFFL	TEA+H2O	TEA-RE	TEA-RE2	TREAFA	UNREAC-G
Phase		Vapor	Vapor	Vapor	Vapor	Liquid	Liquid	Liquid	Liquid	Vapor
C		120	120	120	40	25	37.68	-19.10	307.32	120
bar		100	100	100	22.50	0.20	0.33	0.33	0.33	100
Molar Enthalpy	kcal/mol	0.66	-46.19	-46.20	0.10	-64.81	-67.39	-33.28	-109.21	-46.19
Mass Enthalpy	kcal/kg	326.58	-2008.23	-2008.24	51.22	-2383.62	-3258.13	-328.86	-741.83	-2008.23
Enthalpy Flow	Gcal/hr	0.05	-13.46	-13.46	0.01	-61.86	-59.09	-2.58	-8.47	-13.46
Mole Flow	kmol/hr	78.39	291.27	291.26	78.39	954.55	876.95	77.60	77.60	291.27
Mass Flow	kg/hr	158.02	6699.97	6699.95	158.02	25953.56	18137.47	7852.31	11423.61	6699.97
<b>Mole Fractions</b>										
CO2		0	0.4998	0.4998	0	0	0	0	0	0.4998
H2		1	0.5002	0.5002	1	0	0	0	0	0.5002
O2		0	0	0	0	0	0	0	0	0
N2		0	0	0	0	0	0	0	0	0
CH4		0	0	0	0	0	0	0	0	0
TREA		0	0	0	0	0.1103	0.0307	1.0000	2.31E-10	0
H2O		0	0	0	0	0.8897	0.9684	7.67E-09	7.67E-09	0
HCOOH		0	0	0	0	0	0	0	0	0
NBIM		0	0	0	0	0	0	0	0	0
TREA-FA		0	0	0	0	0	0.0009	0	1.0000	0
NBIM-FA		0	0	0	0	0	0	2.70E-05	0	0
CO		0	0	0	0	0	0	0	0	0

Further technical specifications of major unit operations for the CtX formic acid process are outlined in Tables S3 to S6.

**Table S3.** Technical specifications for B-1 CO<sub>2</sub> hydrogenation reaction.

Operating Conditions	Value	Unit
Model Type	Stoichiometric reactor (R-STOIC)	
Fractional Conversion (CO <sub>2</sub> )	35%	
Temperature	120	°C
Pressure	100	bar
Key Reaction	CO <sub>2</sub> + H <sub>2</sub> + TREA → TREA-Formate	
Net Heat Duty	2099	kW

**Table S4.** Technical specifications for B-2 TREA recovery distillation column.

Operating Conditions	Value	Unit
Model Type	Single-stack fractionation column (RadFrac)	
Number of Stages	5	
Temperature (Condenser)	37.7	°C
Temperature (Reboiler)	307.3	°C
Pressure	0.33	bar
Reflux Ratio (mole-basis)	5	
Bottoms rate to feed rate	0.078	
TREA mole fraction (feed)	2.8 mol. %	
TREA mole fraction (effluent)	Negligible	
Condenser Duty	-68533	kW
Reboiler Heat Duty	68420	kW

**Table S5.** Technical specifications for B-8 Amine exchange reactive distillation column.

Operating Conditions	Value	Unit
Model Type	Single-stack fractionation column (RadFrac)	
Number of Stages	6	
Temperature (Condenser)	-19.1	°C
Temperature (Reboiler)	356.1	°C
Pressure	0.33	bar

Key Reaction	TREA-Formate + <i>n</i> BIM → <i>n</i> BIMH-Formate + TREA	
Fractional Conversion (TEA-Formate)	100%	
Reflux Ratio (mole-basis)	5	
Distillate rate to feed rate	0.5	
Condenser Duty	-6262	kW
Reboiler Heat Duty	5257	kW

**Table S6.** Technical specifications for B-9 formic acid formation and *n*BIM recovery column.

Operating Conditions	Value	Unit
Model Type	Single-stack fractionation column (RadFrac)	
Number of Stages	10	
Temperature (Condenser)	53.6	°C
Temperature (Reboiler)	166.1	°C
Pressure	0.2	bar
Key Reaction	<i>n</i> BIMH-Formate → <i>n</i> BIM + Formic Acid	
Fractional Conversion ( <i>n</i> BIMH-Formate)	100%	
Reflux Ratio (mole-basis)	3	
Distillate rate to feed rate	0.5	
Condenser Duty	-1787	kW
Reboiler Heat Duty	2485	kW

### 3.3. Performance indicator calculation

Two performance indicators- the unit cost of goods manufactured and specific carbon footprint, were selected on a consensus by the CtX formic acid technology stakeholders. Unit COGM, representing economic sustainability, measures the cost of producing one functional unit of a hypothetical *n*<sup>th</sup> plant.<sup>5</sup> In the *n*<sup>th</sup> plant assumption, the current early-stage conceptual process is scaled-up to the commercial-level and multiple iterations of the plant are assumed to co-exist. This allows for the application of heuristic factors for equipment sizes, other direct costs, and indirect costs (such as labor), providing a more realistic end-point cost estimate. Still, uCOGM only serves as an order-of-magnitude estimate and it is primarily used to assess economic feasibility prior to further scale-up.

The unit COGM was calculated by the following equation:

$$\text{Unit COGM} = \frac{\text{Annual CAPEX} + \sum \text{Fixed OPEX} + \sum \text{Variable OPEX}}{\text{Total Annual Production of Functional Unit}} \quad (\text{S5})$$

Variable operating expenses (raw material and utility costs) were estimated from process mass and energy balances. Capital expenses (CAPEX) were estimated by the method presented in Towler and Sinnott.<sup>6</sup> Direct and indirect capital costs were estimated by applying Lang factors to the total installed equipment cost. The Lang factor for working capital was subsequently applied to the sum of direct and indirect capital costs. Annual capital expenses, which are the payments of borrowed capital (principal + interest) to investors, was subsequently calculated by multiplying the capital recovery factor (CRF) by the total capital expenditure.

$$\text{Installed Equipment Cost (IEC)} = (1 + f^{IEC}) \cdot \sum \text{Equipment Cost} \quad (\text{S6})$$

$$\text{Direct Capital Cost (DCC)} = (1 + f^{DCC}) \cdot \text{IEC} \quad (\text{S7})$$

$$\text{Indirect Capital Cost (ICC)} = (1 + f^{ICC}) \cdot \text{IEC} \quad (\text{S8})$$

$$\text{Total Capital Expenditure} = (1 + f^{WC}) \cdot (\text{DCC} + \text{ICC}) \quad (\text{S9})$$

$$\text{Capital Recovery Factor} = \frac{d(d+1)^{LT}}{(d+1)^{LT} - 1} \quad (\text{S10})$$

$$\text{Labor} = 1,135,836 \text{ USD} \cdot \frac{\text{Current Plant Capacity}}{200 \text{ tons FA/yr}} \quad (\text{S11})$$

$$\text{Maintenance} = f^{MNT} \cdot \text{IEC} \quad (\text{S12})$$

$$\text{Admin} = f^{ADM} \cdot \text{Labor} \quad (\text{S13})$$

$$\text{Overhead} = f^{OH} \cdot \text{Labor} \quad (\text{S14})$$

$$\text{Laboratory} = f^{LB} \cdot \text{IEC} \quad (\text{S15})$$

Fixed operating expenses were estimated in a similar manner by applying appropriate Lang factors. Labor, maintenance, admin, overhead, and laboratory were considered. Labor was estimated from the bottom-up based on estimated personnel for a reference 200 ton/yr formic acid demonstration plant (Table S7). Base salaries were referenced from Davis *et al.*<sup>7</sup> and corrected for inflation. Lang factors for capital and fixed operating expenses were provided by the CtX stakeholders. A summary of relevant techno-economic assessment parameters is provided in Table S8.

**Table S7.** Labor requirements for a reference 200 ton/yr formic acid demonstration plant. Salaries were referenced from Davis *et al.* accounting for inflation.

Position	Number Required	2021 Salary (USD)	Labor Cost
Plant Manager	1	182,072	182,072
Maintenance Supervisor	1	70,599	70,599
Technician	2	49,544	99,088
Lab Manager	1	69,361	69,361
Lab Technician	2	49,544	99,088
Shift Supervisor	4	59,452	237,808
Process Operators	12	31,485	377,820
<b>Total</b>	<b>23</b>	<b>512,057</b>	<b>1,135,836</b>

**Table S8.** Techno-economic analysis parameters for the calculation of unit COGM indicator.

Parameter	Value
Equipment installation factor, $f^{IEC}$	0.1
Direct capital cost factor, $f^{DCC}$	0.44
Indirect capital cost factor, $f^{ICC}$	0.6
Working capital factor, $f^{WC}$	0.05
Maintenance cost factor, $f^{MNT}$	0.03
Administration cost factor, $f^{ADM}$	0.2
Overhead cost factor, $f^{OH}$	0.6
Laboratory cost factor, $f^{LB}$	0.01
Discount factor (interest rate), $d$	0.07
Plant lifetime, $LT$ , years	30

The specific carbon footprint indicator (ton-CO<sub>2</sub>eq/ton) measures the cradle-to-gate greenhouse gas emissions as a result of operating the CtX formic acid process. To measure this indicator, an

attributional CO<sub>2</sub> life cycle assessment was performed utilizing average impact data.<sup>8</sup> Emission factors for raw materials and utilities corresponding to South Korea, where the plant is to be located, were estimated on the basis of GWP<sub>20</sub> wherever possible. An exception was the emission factor for captured CO<sub>2</sub>, for which location-independent literature values were used. Significant emission factors were considered as sources of exogenous sustainability risk (Table S9). In this study, we focused solely on emissions incurred during operation, which meant that indirect impacts from plant construction and salvage were not included. A schematic showing the system boundary is shown in Figure S3.

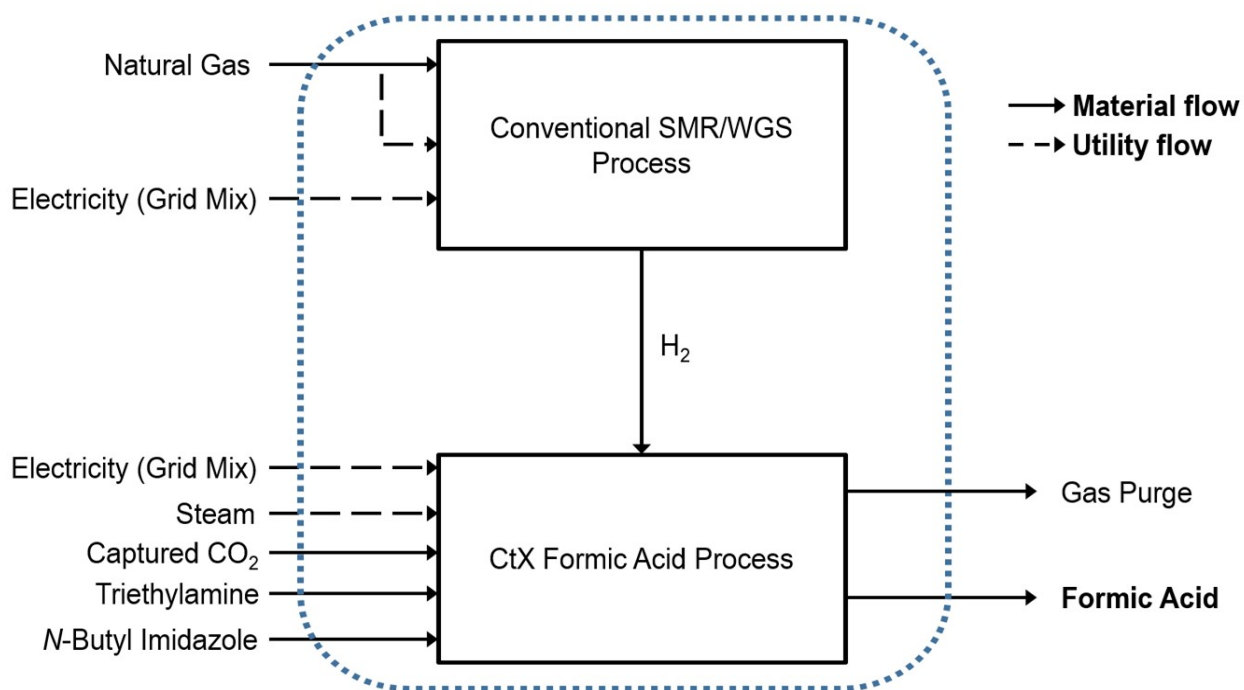


**Figure S3.** System boundary for the CO<sub>2</sub> life cycle assessment of the CtX formic acid process.

Consistent with the above description, the specific carbon footprint indicator was calculated by the following equation:

$$\text{Specific Carbon Footprint} = \frac{\sum \text{Direct Emissions} + \sum \text{Indirect Emissions}}{\text{Total Annual Production of Functional Unit}} \quad (\text{S16})$$

### 3.4. Validation of COSMO-RS VLE data

VLE data between the amines (triethylamine, and *n*-butyl imidazole), water, and formate is required to estimate binary interaction parameters which are used to simulate separation processes. The Universal Quasi-Chemical (UNIQUAC) activity coefficient model was assumed and COSMO-RS<sup>TM</sup> was used to generate the necessary VLE data. The UNIQUAC model was validated with experimental data as shown in Figure S4.

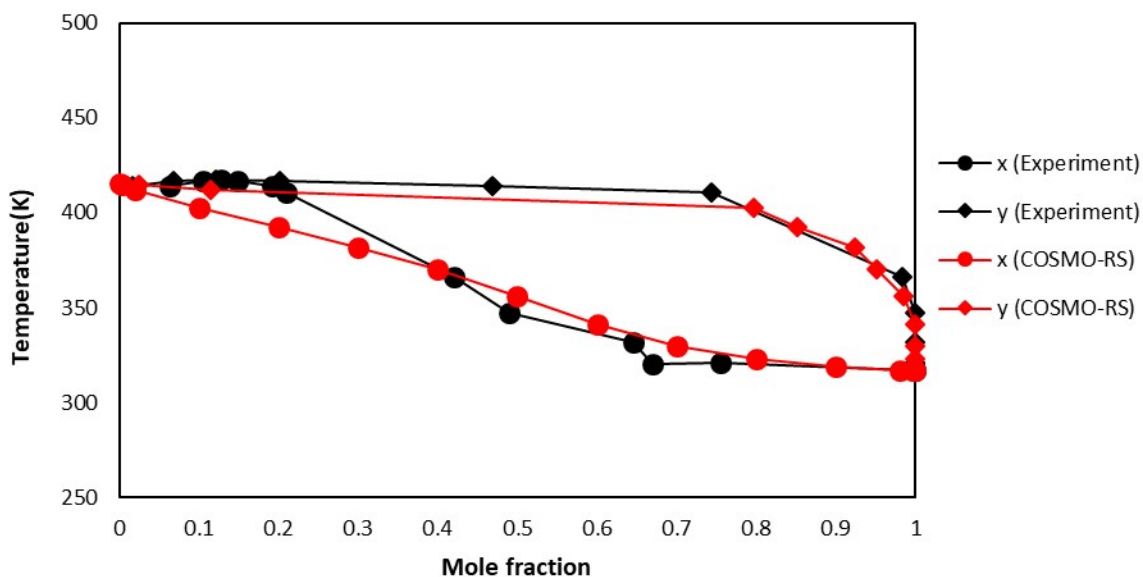


**Figure S4.** Experimental validation of VLE data for *n*-butylimidazole and formate adduct simulated using COSMO-RS<sup>TM</sup>.

### 3.5. Prior distribution data for uncertain inputs

**Table S9.** Kernel data points for the prior distribution of key uncertainties with data sources.

Uncertainties	Unit	Region	Kernel Data points	Method	Source
TBR CO <sub>2</sub> conversion		N/A	0.638, 0.669, 0.411, 0.656, 0.333, 0.133, 0.583, 0.545, 0.448, 0.569, 0.546, 0.501, 0.436, 0.480, 0.457, 0.429, 0.368, 0.479	Experimental CO <sub>2</sub> conversion data from TBR at 120°C and 120 bar	9
TREA degradation		N/A	0.08, 0.1, 0.125	Assumed loss rate of 10% with ±25% error bars	***
nBIM degradation		N/A	0.08, 0.1, 0.125	Assumed loss rate of 10% with ±25% error bars	***
Korean grid mix electricity price	USD/GJ <sub>e</sub>	Korea	Off Peak*: 13.41, 13.40, 15.08 Mid-Load*: 25.89, 18.73, 25.89, 25.49, 18.35, 25.49 Peak Load*: 45.27, 25.96, 39.30	Data corresponds to “High Voltage B” (industrial). Prices varied between regional vendors (Chungnam, Gyeonggi, and Kyungpuk)	10
Korean steam price ( <i>industrial, &gt; 43000 GJ/yr</i> )	USD/GJ	Korea	Winter**: 19.03 <sup>b</sup> , 18.92 <sup>c</sup> , 17.81 <sup>a</sup> Summer**: 16.63 <sup>a</sup> , 17.85 <sup>b</sup> , 17.75 <sup>c</sup> Other**: 17.81 <sup>c</sup> , 16.69 <sup>a</sup> , 17.91 <sup>b</sup> ,	Rates for large scale industrial heating (“industrial class 1”) for winter, summer, and off-season months	a <sup>11</sup> b <sup>12</sup> c <sup>13</sup>
Korean natural gas price	USD/ton	Korea	Winter**: 268.63 <sup>a</sup> , 287.04 <sup>b</sup> , 285.52 <sup>c</sup> Summer**: 250.81 <sup>a</sup> , 269.24 <sup>b</sup> , 267.73 <sup>c</sup> Other**: 251.87 <sup>a</sup> , 270.27 <sup>b</sup> , 268.76 <sup>c</sup>	Prices corresponding to three regional natural gas vendors for industrial-scale application. Includes customs and import tax.	a <sup>14</sup> b <sup>12</sup> c <sup>13</sup>
Captured CO <sub>2</sub> price ( <i>from power plants</i> )	USD/ton	Global	40, 60, 80	Min, Mean, and Max values of levelized cost of CO <sub>2</sub> capture from power generation plants	15

\* Off-peak hours correspond to 23:00 – 7:00. Mid load corresponds to 9:00 – 10:00, 12:00 – 13:00, 17:00 – 23:00. Peak load corresponds to 7:00 – 9:00, 10:00 – 12:00, 13:00 – 17:00

\*\* Winter months correspond to December – March. Summer months correspond to June - August

\*\*\* Detailed references could not be included due to information confidentiality

**Table S9.** Kernel data points for the prior distribution of key uncertainties with data sources. (continued)

Uncertainties	Unit	Region	Kernel Data points	Method	Source
TREA price	USD/ton	Asia	2544, 1500, 2200, 2150, 2390	Wholesale quotes from multiple regional vendors	
nBIM price	USD/ton	Asia	8000, 4000, 10000	Wholesale quotes from multiple regional vendors	
Emission factor for captured CO <sub>2</sub>	Ton-CO <sub>2</sub> eq/ton	Global	-0.8 <sup>a</sup> , -0.86 <sup>b</sup> , -0.8 <sup>c</sup> , -0.67 <sup>d</sup>	Short-term global warming impact of captured CO <sub>2</sub> from power plants based on market mix.	a <sup>16</sup> b <sup>17, 18</sup> c <sup>19</sup> d <sup>20</sup>
Emission factor for Korean grid mix electricity production	Ton-CO <sub>2</sub> eq/GJ <sub>e</sub>	Korea	0.185 <sup>a</sup> , 0.154 <sup>a</sup> , 0.129 <sup>b</sup> , 0.138 <sup>c</sup>	Normalized global warming impact of the South Korean electricity grid.	a <sup>***</sup> b <sup>21</sup> c <sup>22</sup>
Emission factor for industrial steam production	Ton-CO <sub>2</sub> eq/GJ	Korea	0.069 <sup>a</sup> , 0.089 <sup>b</sup> , 0.060 <sup>c</sup>	Steam production from natural gas boilers a- Korean Ministry of Commerce Industry and Energy (ca. 2003) b- Korean Ministry of Environment (2016)	c <sup>22</sup>
Emission factor for Korean natural gas production	Ton-CO <sub>2</sub> eq/ton	Korea	0.301 <sup>a</sup> , 0.614 <sup>a</sup> , 0.102 <sup>b</sup>	a- Natural gas production, compression, and transport b- Landfill gas	***
Emission factor for Korean process water production	Ton-CO <sub>2</sub> eq/m <sup>3</sup>	Global	1.73E-4 <sup>a</sup> , 1.99E-4 <sup>a</sup> , 1.23E-4 <sup>b</sup>	Treatment and supply of aquifer water for process applications	a <sup>***</sup> b <sup>22</sup>

\* Off-peak hours correspond to 23:00 – 7:00. Mid load corresponds to 9:00 – 10:00, 12:00 – 13:00, 17:00 – 23:00. Peak load corresponds to 7:00 – 9:00, 10:00 – 12:00, 13:00 – 17:00

\*\* Winter months correspond to December – March. Summer months correspond to June - August

\*\*\* Detailed references could not be included due to information confidentiality

**Table S10.** Lower and upper bounds for prior distributions defined by KDE method.

Uncertain Input		Lower Bound	Upper Bound
TBR CO <sub>2</sub> conversion, %	$x_{j=1}$	0.1	1
TREA degradation, %	$x_2$	0	1
<i>n</i> BIM degradation, %	$x_3$	0	1
Korean grid mix electricity price, USD/GJ <sub>e</sub>	$x_4$	0	100
Korean industrial steam price, USD/GJ	$x_5$	0	100
Korean natural gas price, USD/ton	$x_6$	0	1,000
Price of captured CO <sub>2</sub> (power plants), USD/ton	$x_7$	0	500
Price of TREA, USD/ton	$x_8$	100	50,000
Price of <i>n</i> BIM, USD/ton	$x_9$	100	100,000
Emission factor for captured CO <sub>2</sub> , ton-CO <sub>2</sub> eq/ton	$x_{10}$	-1	0
Emission factor for Korean grid mix electricity production, ton-CO <sub>2</sub> eq/ton	$x_{11}$	0	10
Emission factor for Korean industrial steam production, ton-CO <sub>2</sub> eq/ton	$x_{12}$	0	10
Emission factor for Korean natural gas production, ton-CO <sub>2</sub> eq/ton	$x_{13}$	0	10
Emission factor for process water, ton-CO <sub>2</sub> eq/ton	$x_{14}$	0	1

### 3.6. Convergence plot for Monte Carlo simulations

Figure S5 displays the convergence plot which compares the coefficient of variation for  $P(D = "S")$  in both individual criteria ( $f^{uCOGM}$ ,  $f^{CF}$ ) and multi-criteria scenarios.

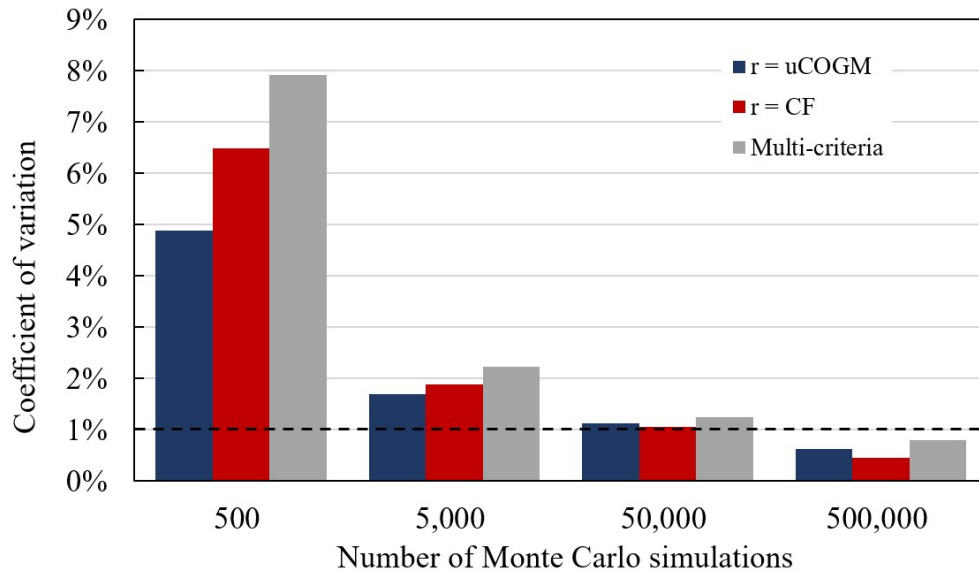


**Figure S5.** Coefficient of variation with respect to  $P(D = "S")$  at varying Monte Carlo simulation numbers. The convergence criteria was set to  $\leq 1\%$  coefficient of variation.

### 3.7. Class likelihood distributions for uncertain inputs

Figures S6 to S19 displays the class likelihood distributions estimated by KDE for individual criteria (considering the unit COGM and specific carbon footprint criteria separately). Figures S20 to S33 displays the class likelihood distributions for the multi-criteria case.

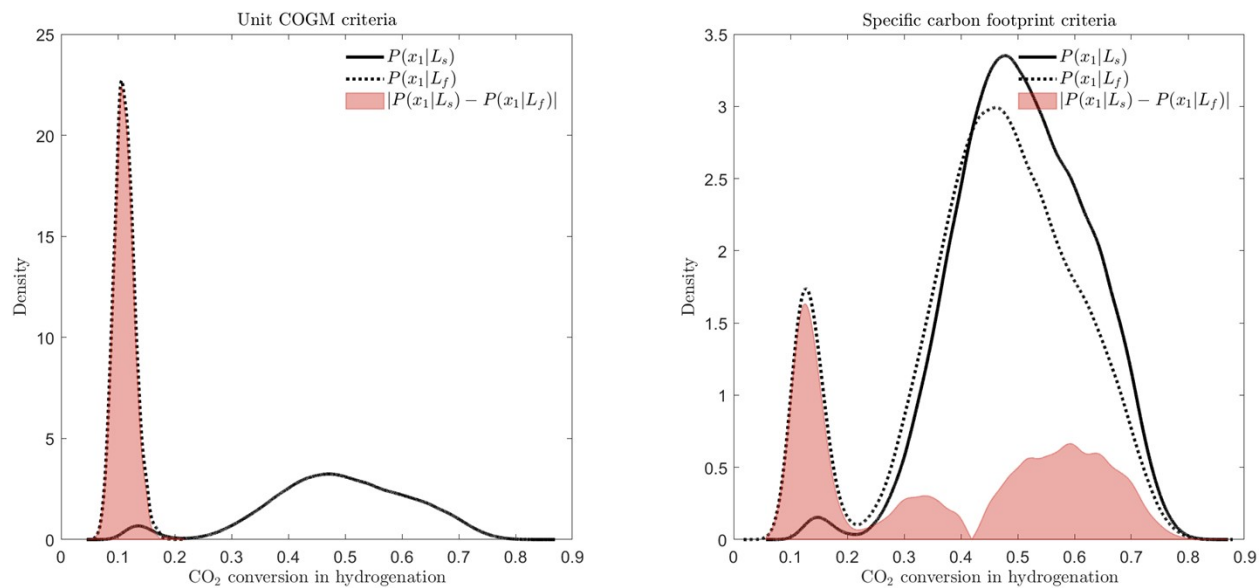


**Figure S6.** Class likelihood distributions for the CO<sub>2</sub> conversion parameter ( $x_1$ ), individual criteria.

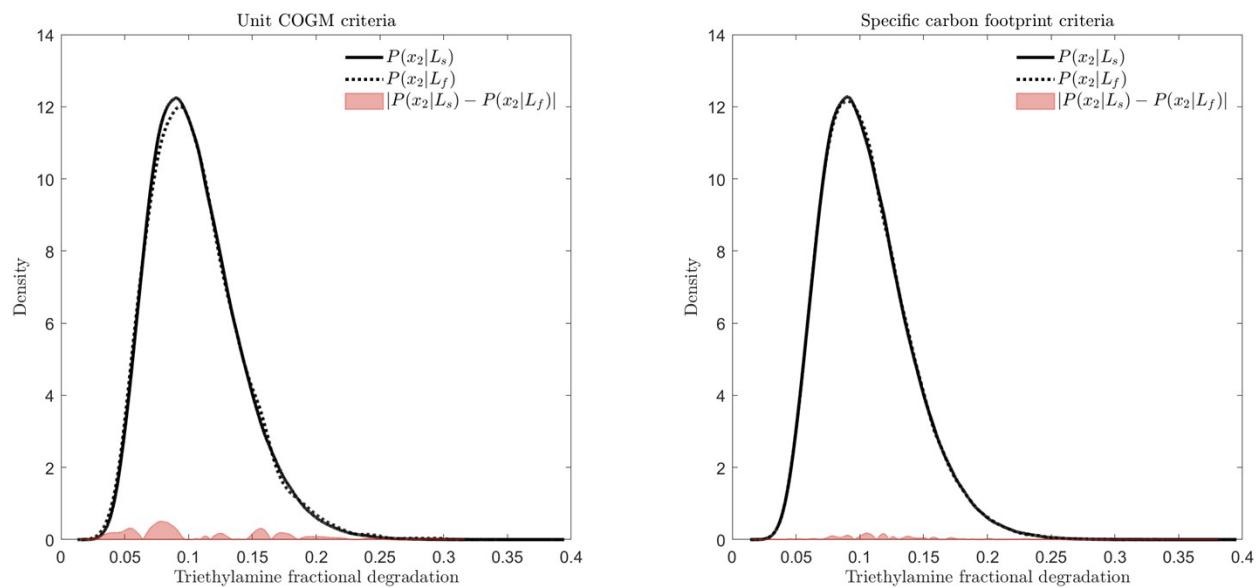


**Figure S7.** Class likelihood distributions for the TREA fractional degradation parameter ( $x_2$ ), individual criteria.

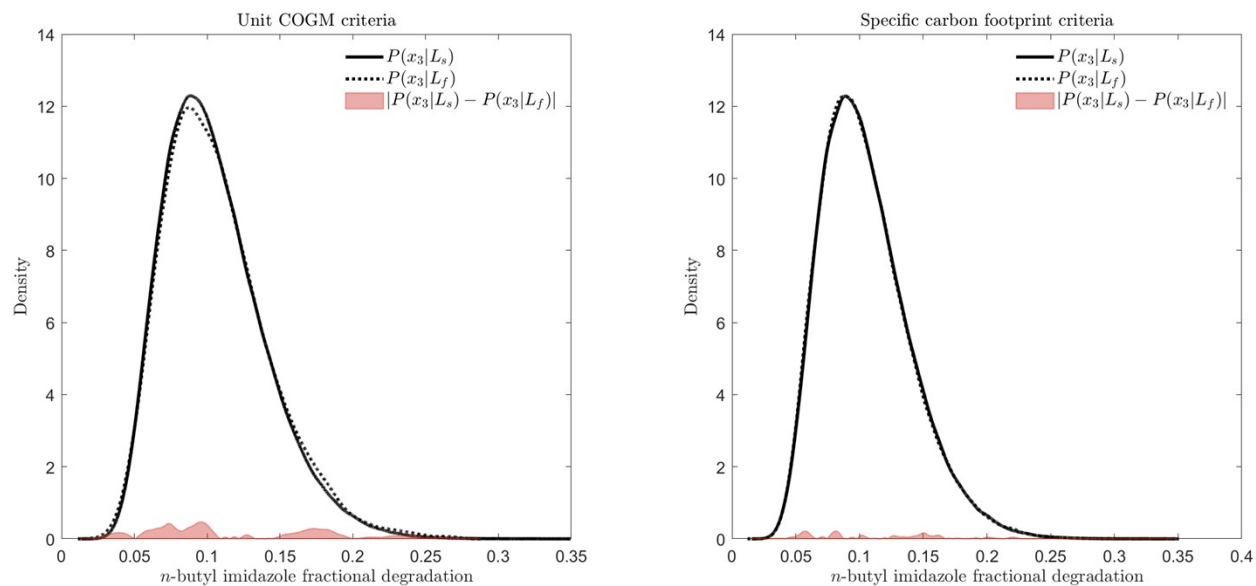


**Figure S8.** Class likelihood distributions for the  $n$ BIM fractional degradation parameter ( $x_3$ ), individual criteria.

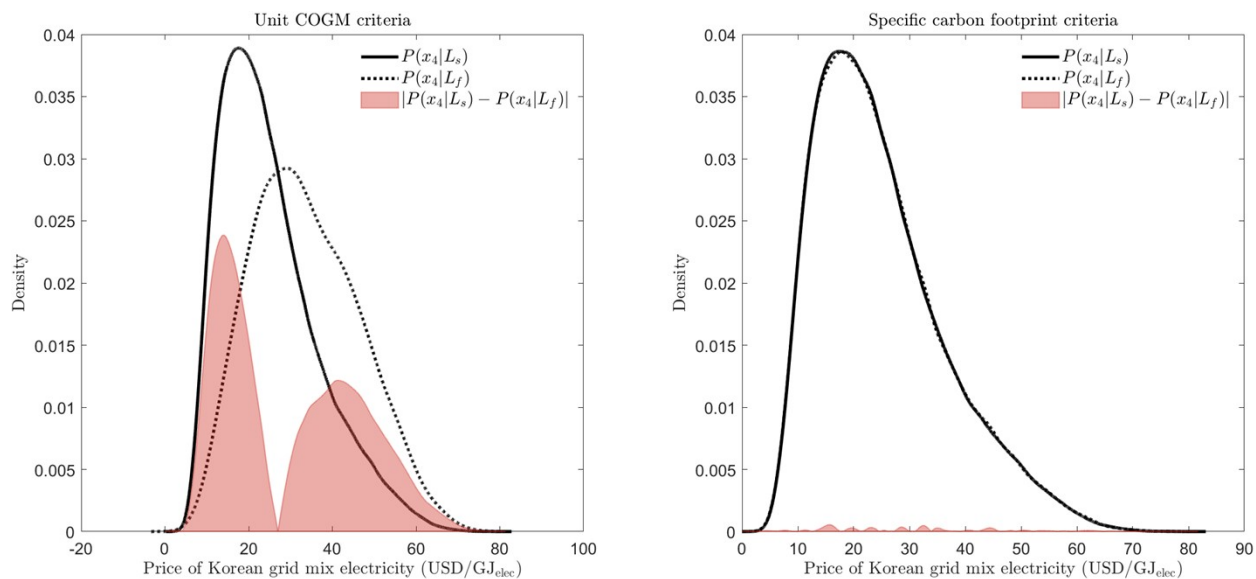


**Figure S9.** Class likelihood distributions for the price of Korean grid mix electricity ( $x_4$ ), individual criteria.

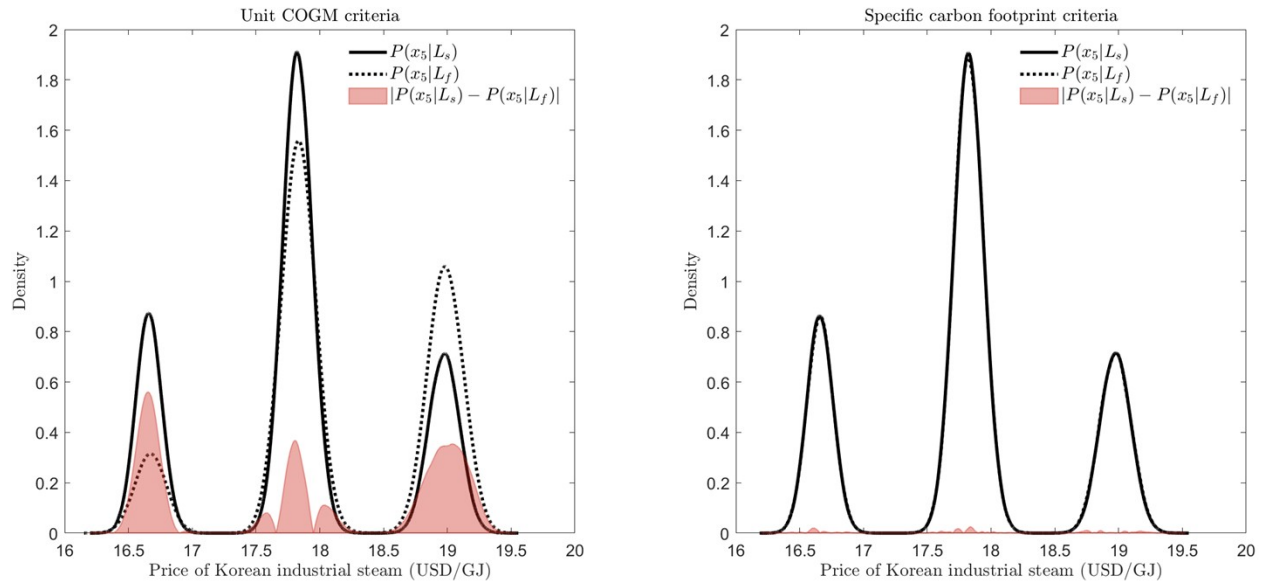


**Figure S10.** Class likelihood distributions for the price of Korean industrial steam ( $x_5$ ), individual criteria.

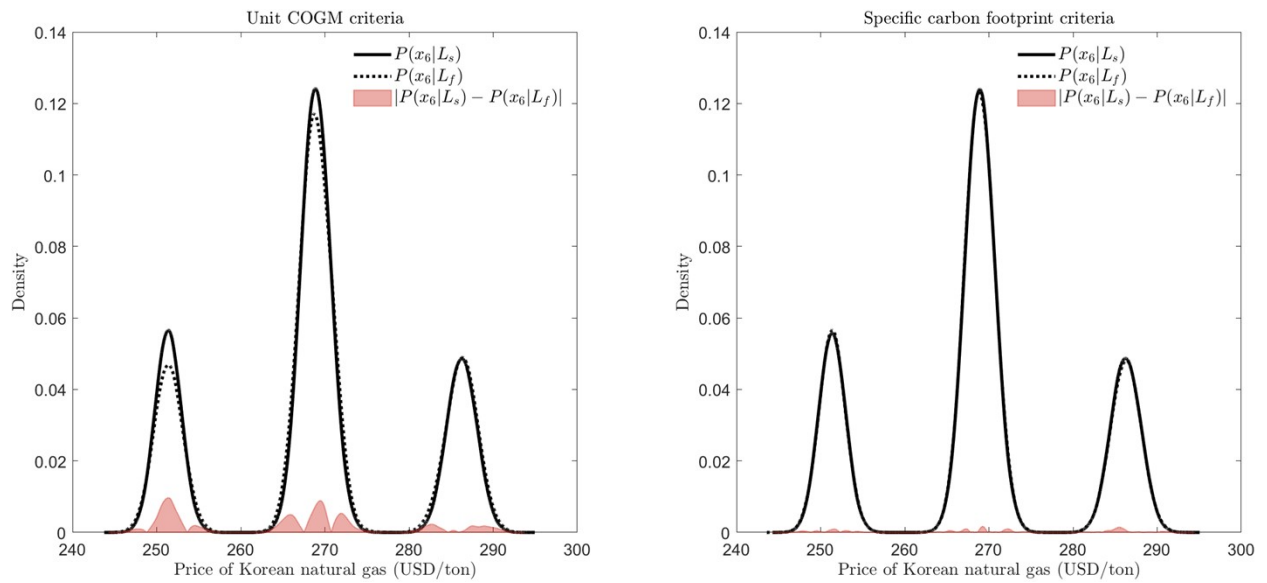


**Figure S11.** Class likelihood distributions for the price of Korean natural gas ( $x_6$ ), individual criteria.

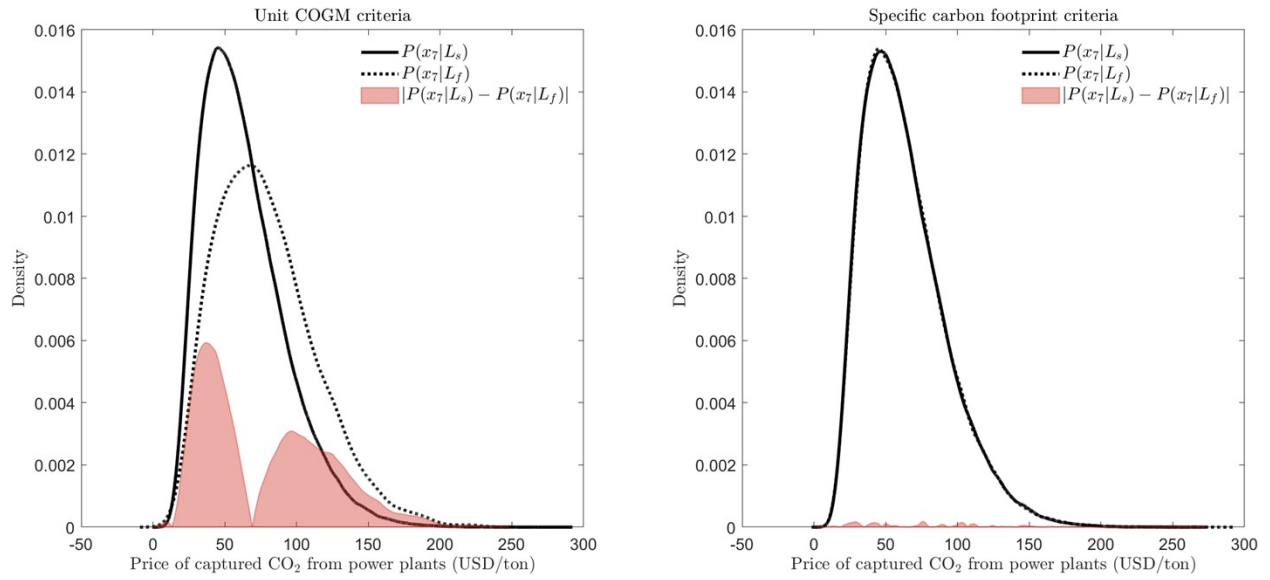


**Figure S12.** Class likelihood distributions for the price of captured CO<sub>2</sub> from power plants ( $x_7$ ), individual criteria.

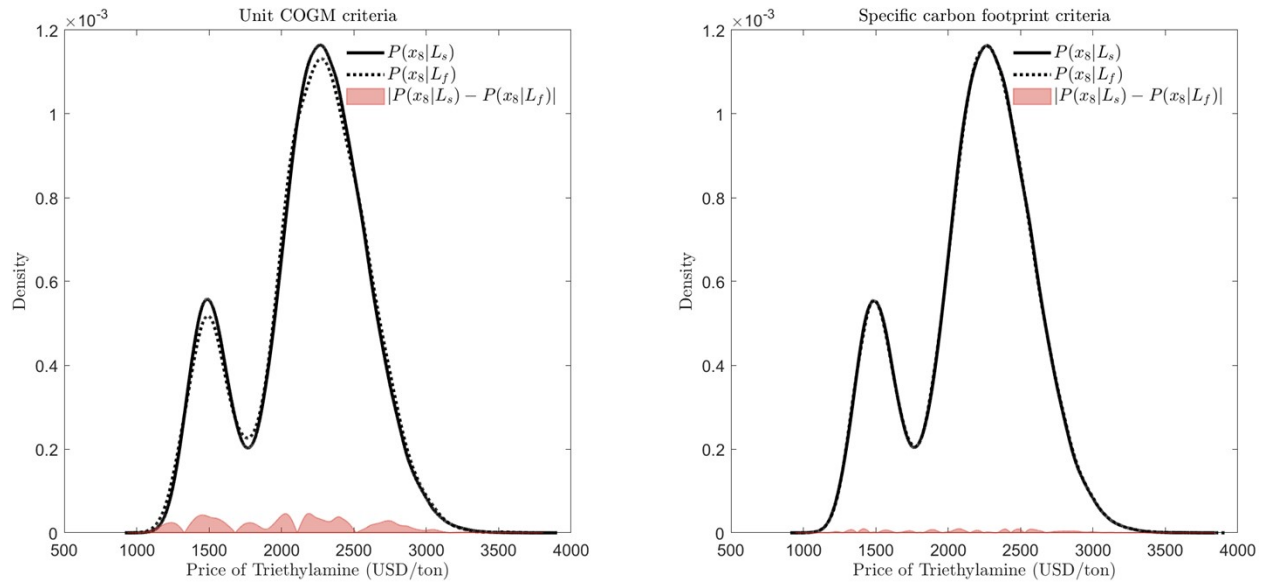


**Figure S13.** Class likelihood distributions for the price of Triethylamine ( $x_8$ ), individual criteria.

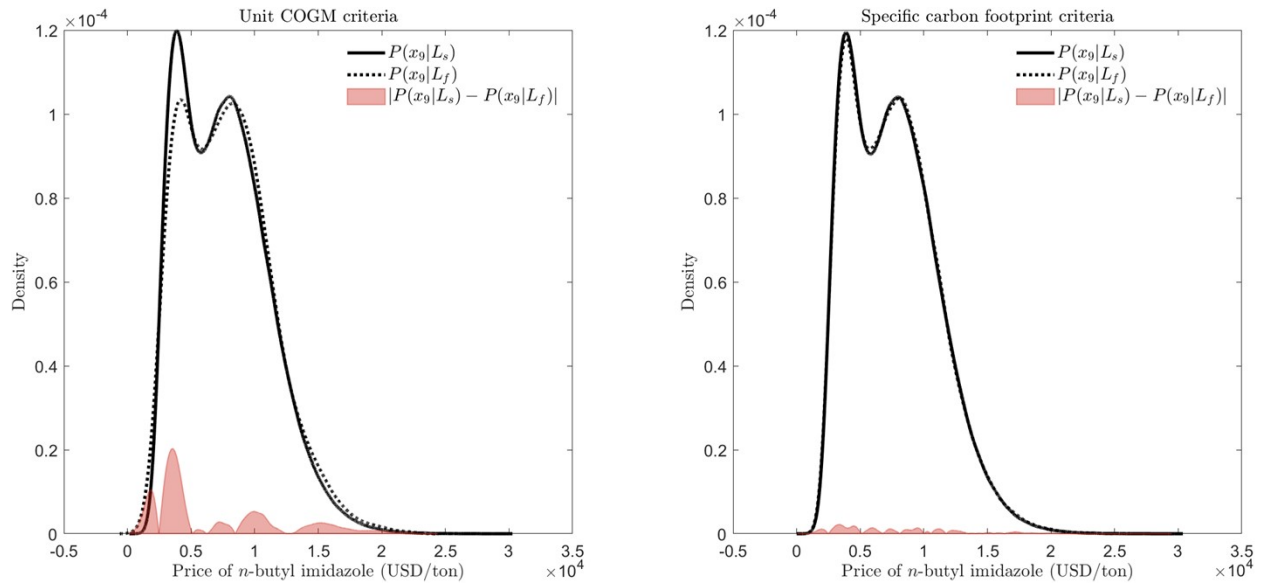


**Figure S14.** Class likelihood distributions for the price of *n*-butyl imidazole ( $x_9$ ), individual criteria.

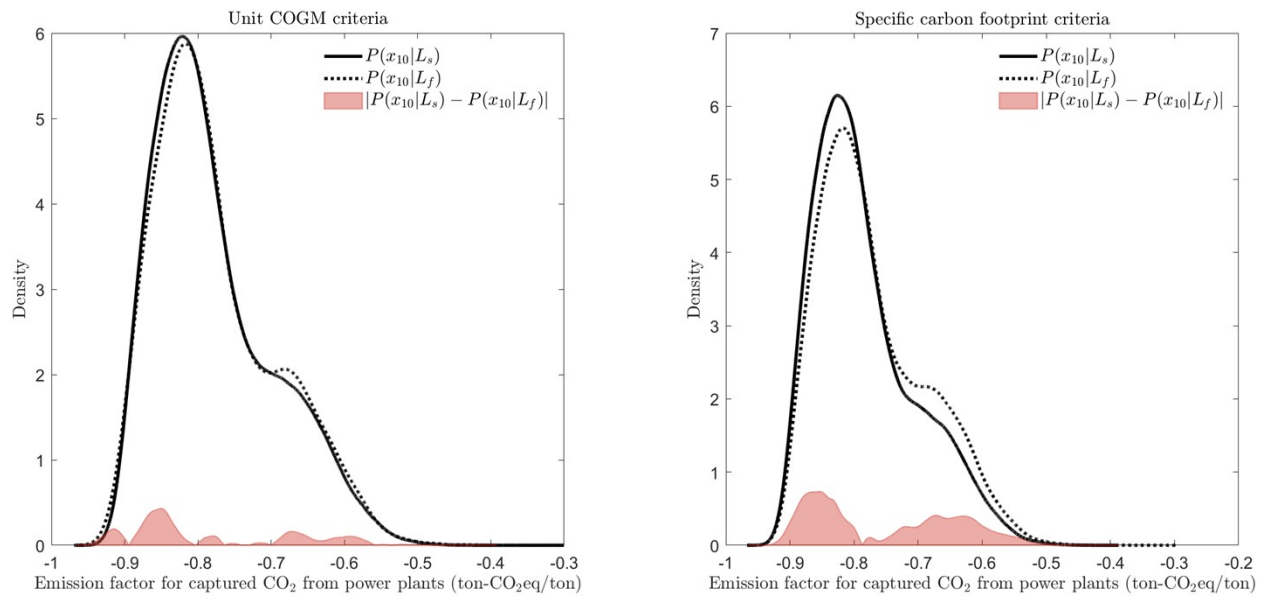


**Figure S15.** Class likelihood distributions for the emission factor of captured CO<sub>2</sub> ( $x_{10}$ ), individual criteria.

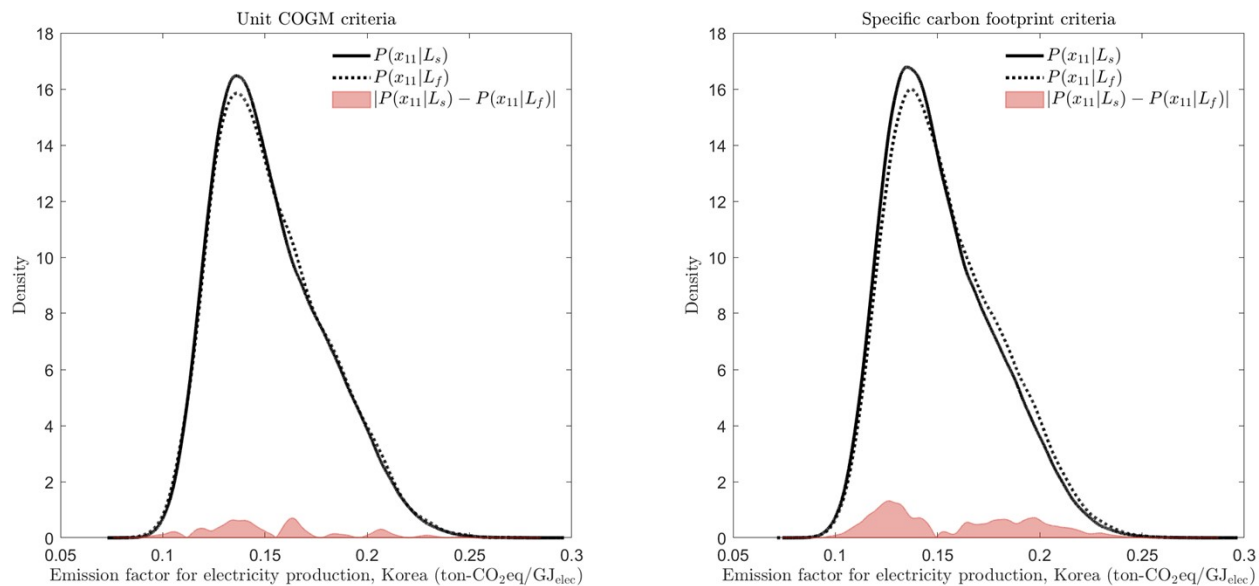


**Figure S16.** Class likelihood distributions for emission factor of Korean grid mix electricity generation ( $x_{11}$ ), individual criteria.

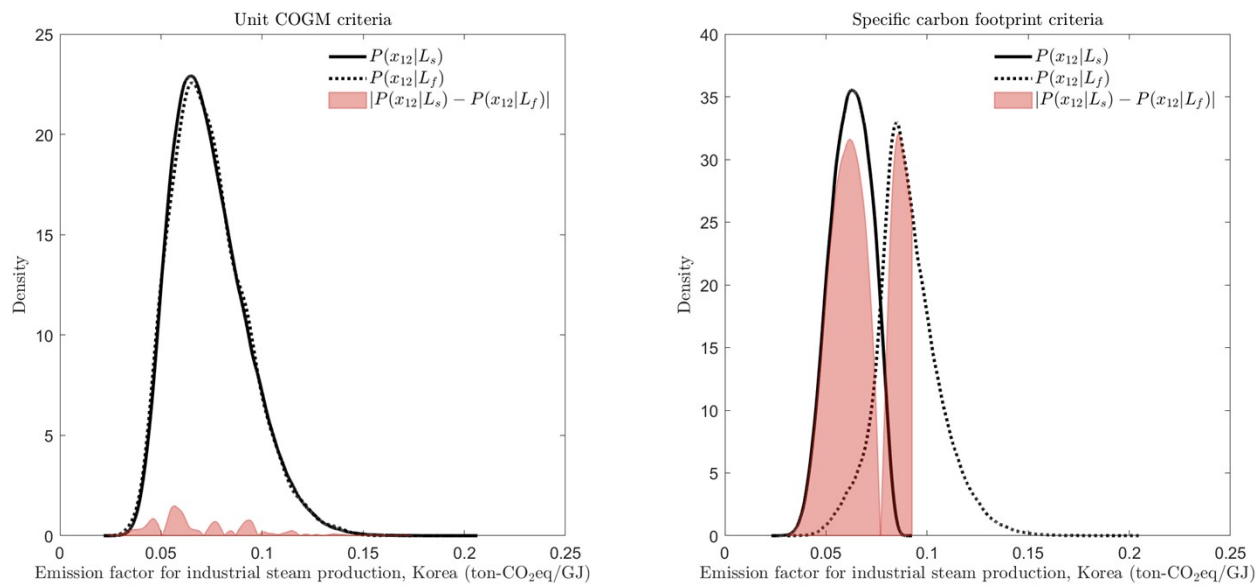


**Figure S17.** Class likelihood distributions for the emission factor of Korean industrial steam generation ( $x_{12}$ ), individual criteria.

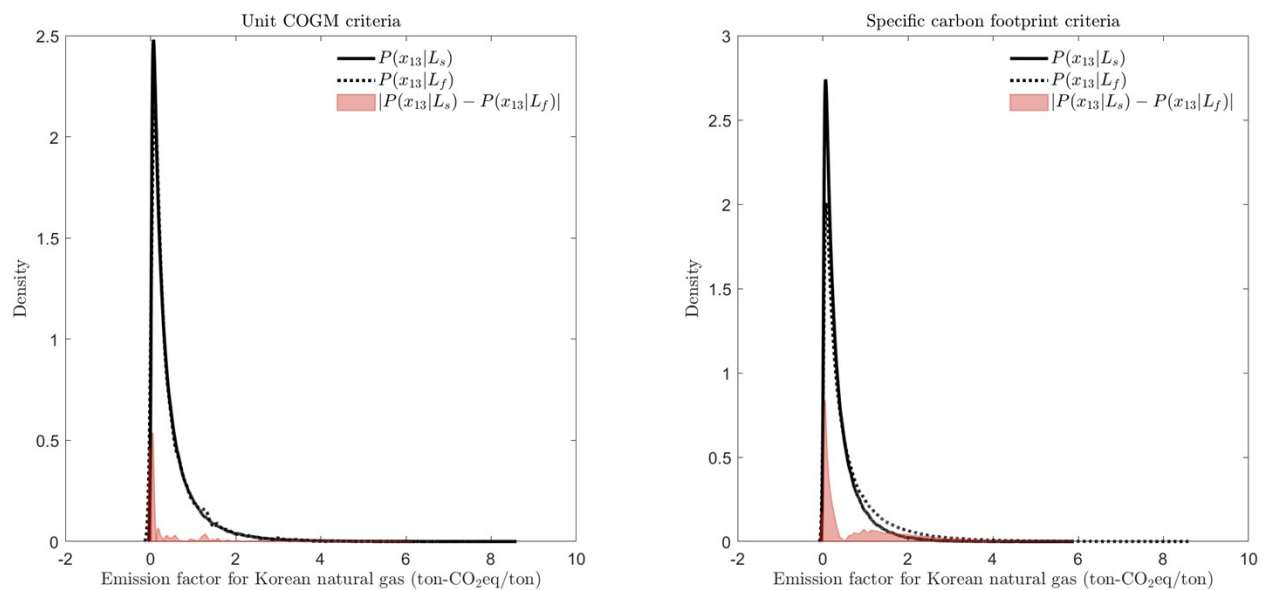


**Figure S18.** Class likelihood distributions for the emission factor of Korean natural gas ( $x_{13}$ ), individual criteria.

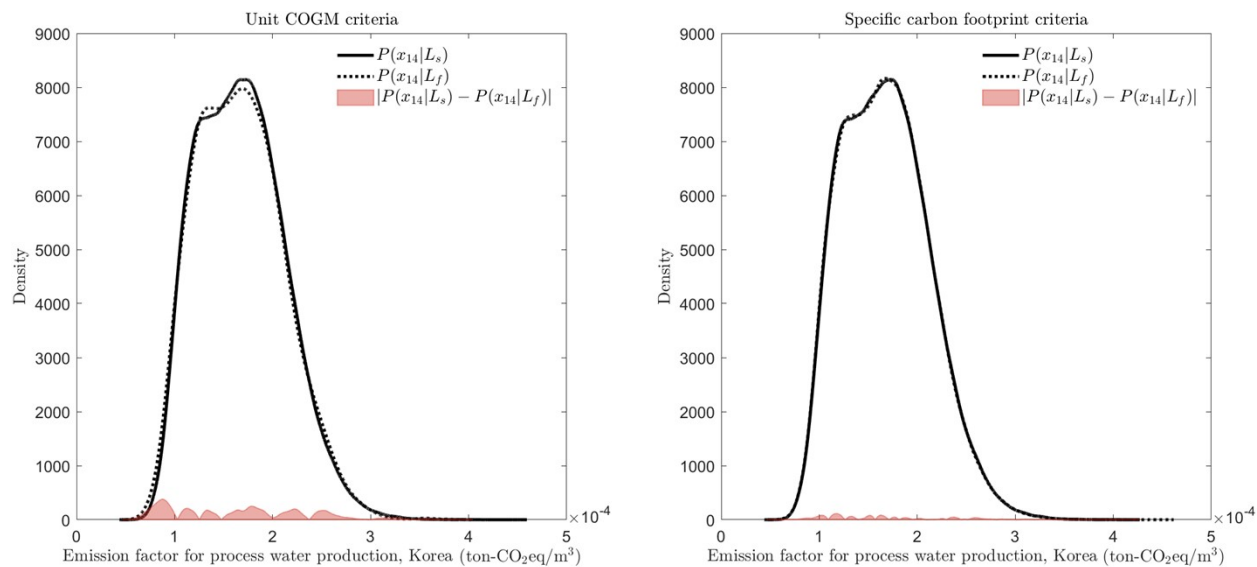


**Figure S19.** Class likelihood distributions for the emission factor of Korean process water production and supply ( $x_{14}$ ), individual criteria.

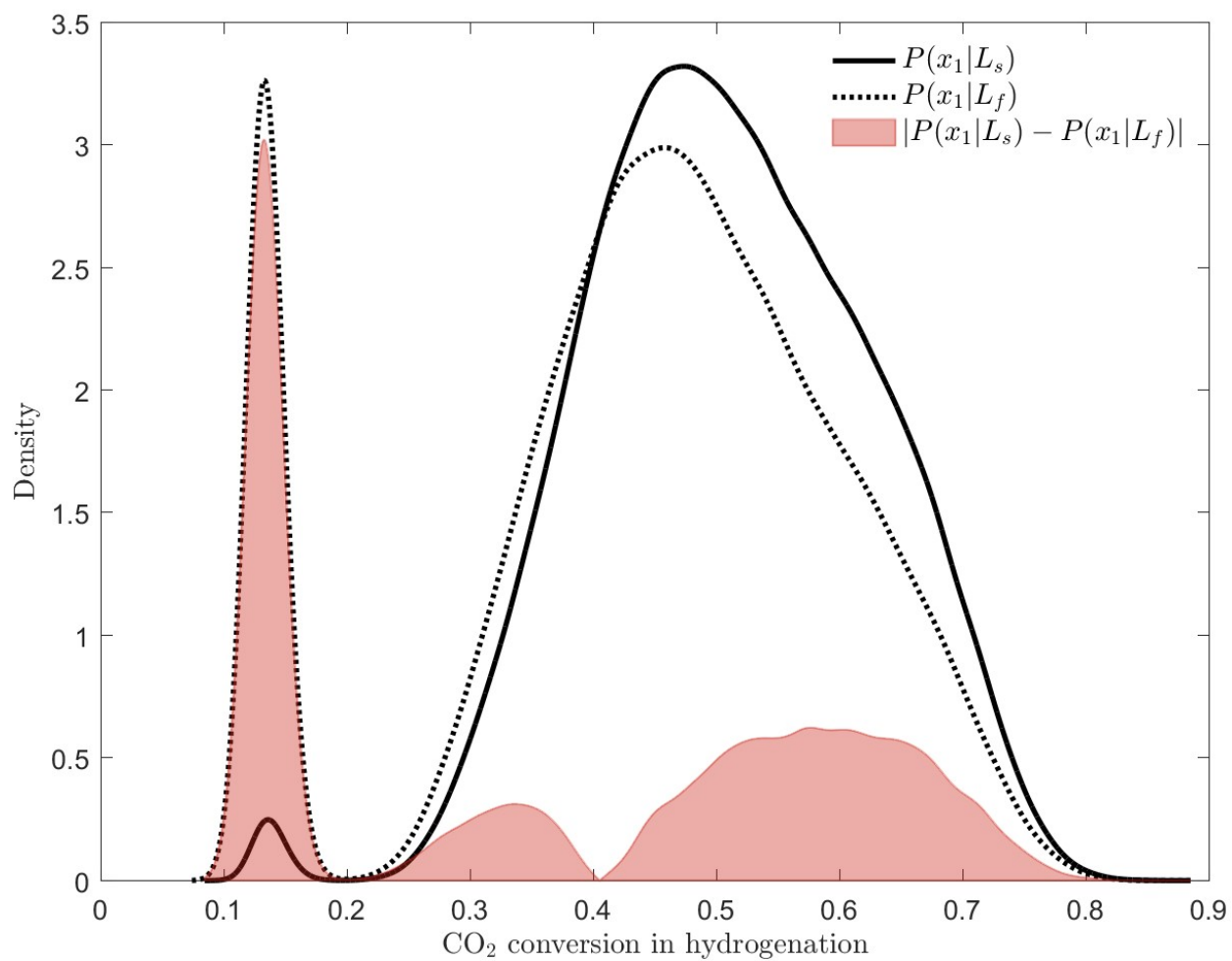


**Figure S20.** Likelihood distribution for CO<sub>2</sub> conversion parameter ( $x_1$ ), multi-criteria.

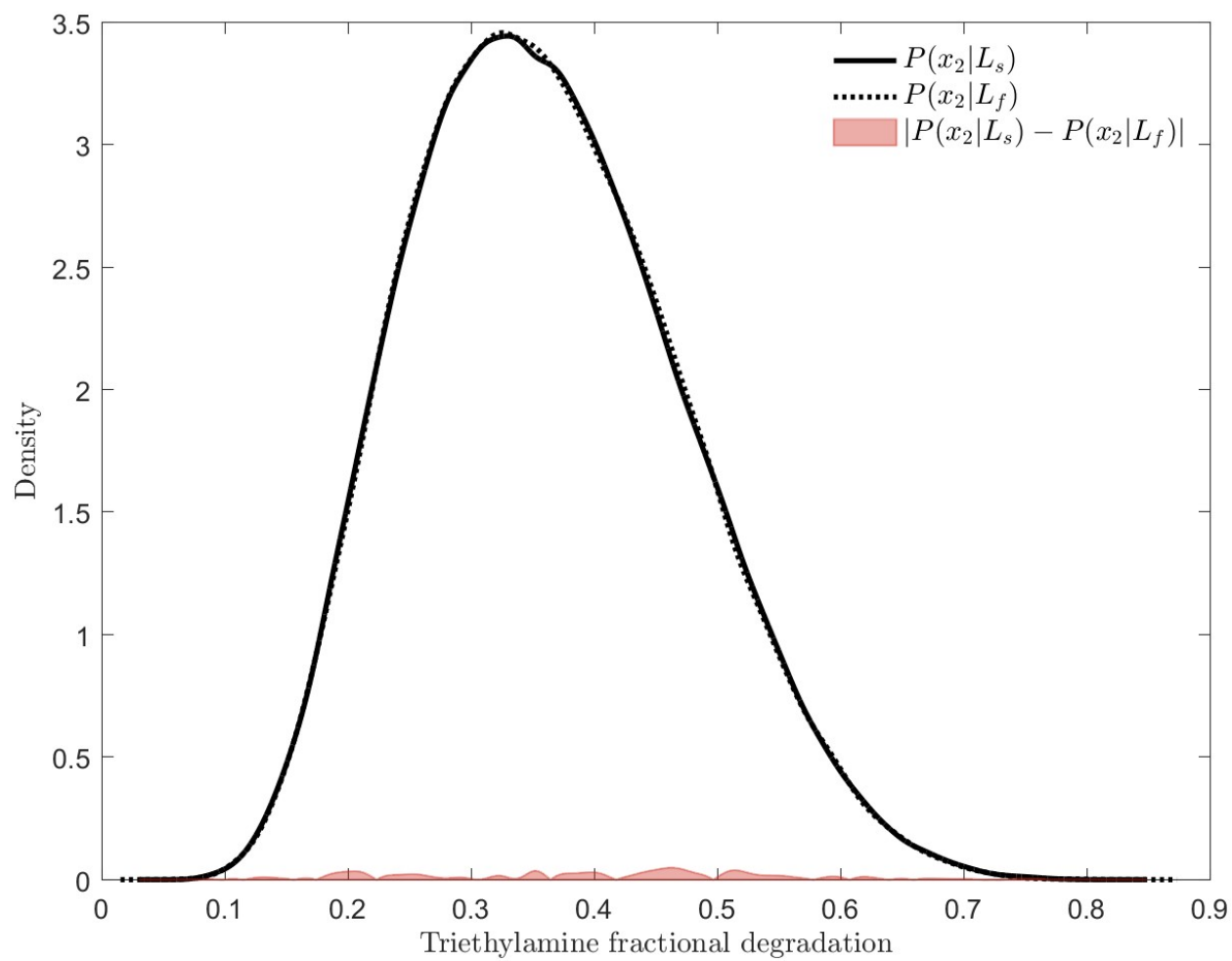


**Figure S21.** Likelihood distribution for TEA fractional degradation parameter ( $x_2$ ), multi-criteria.

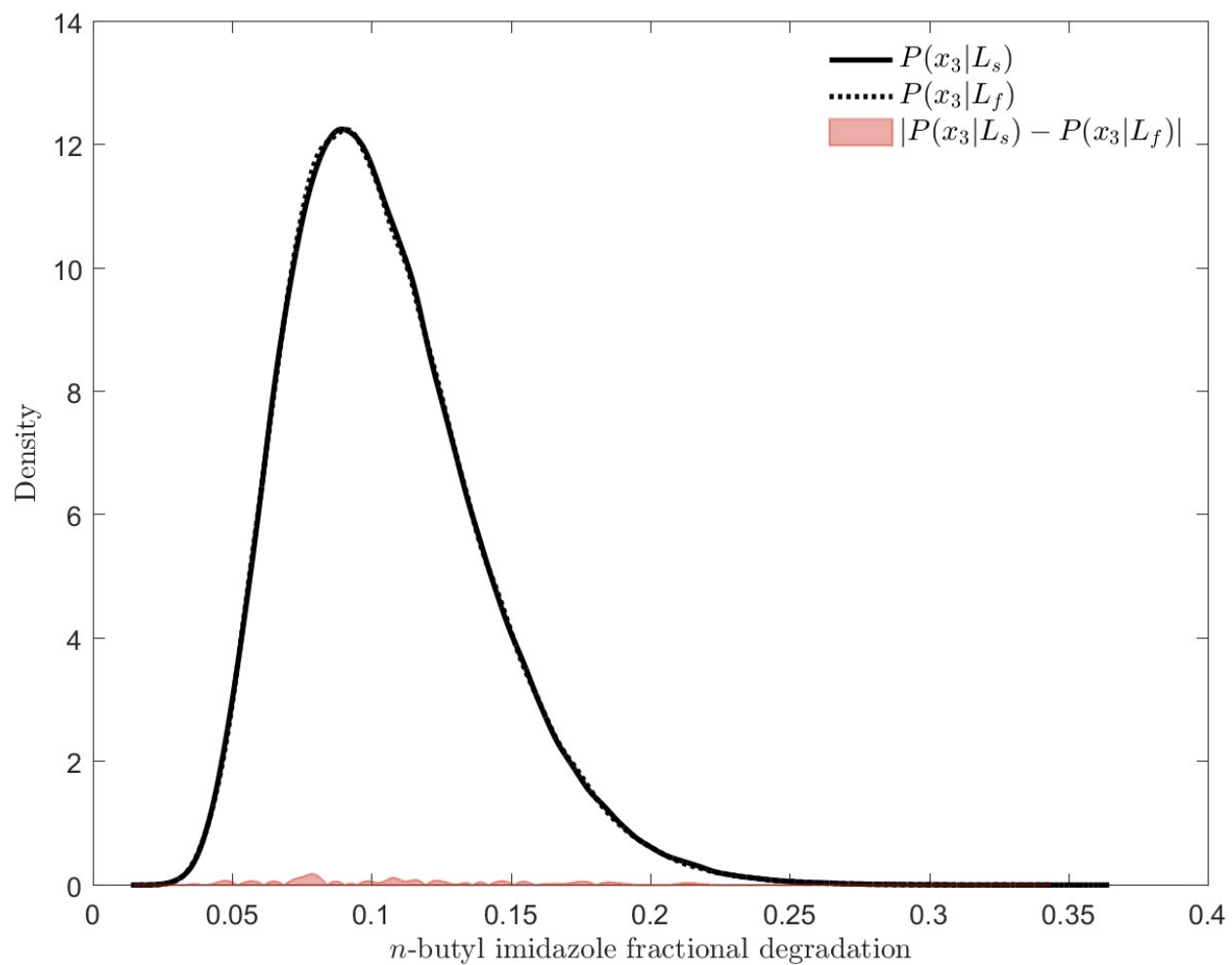


**Figure S22.** Likelihood distribution for  $n$ BIM fractional degradation parameter ( $x_3$ ), multi-criteria.

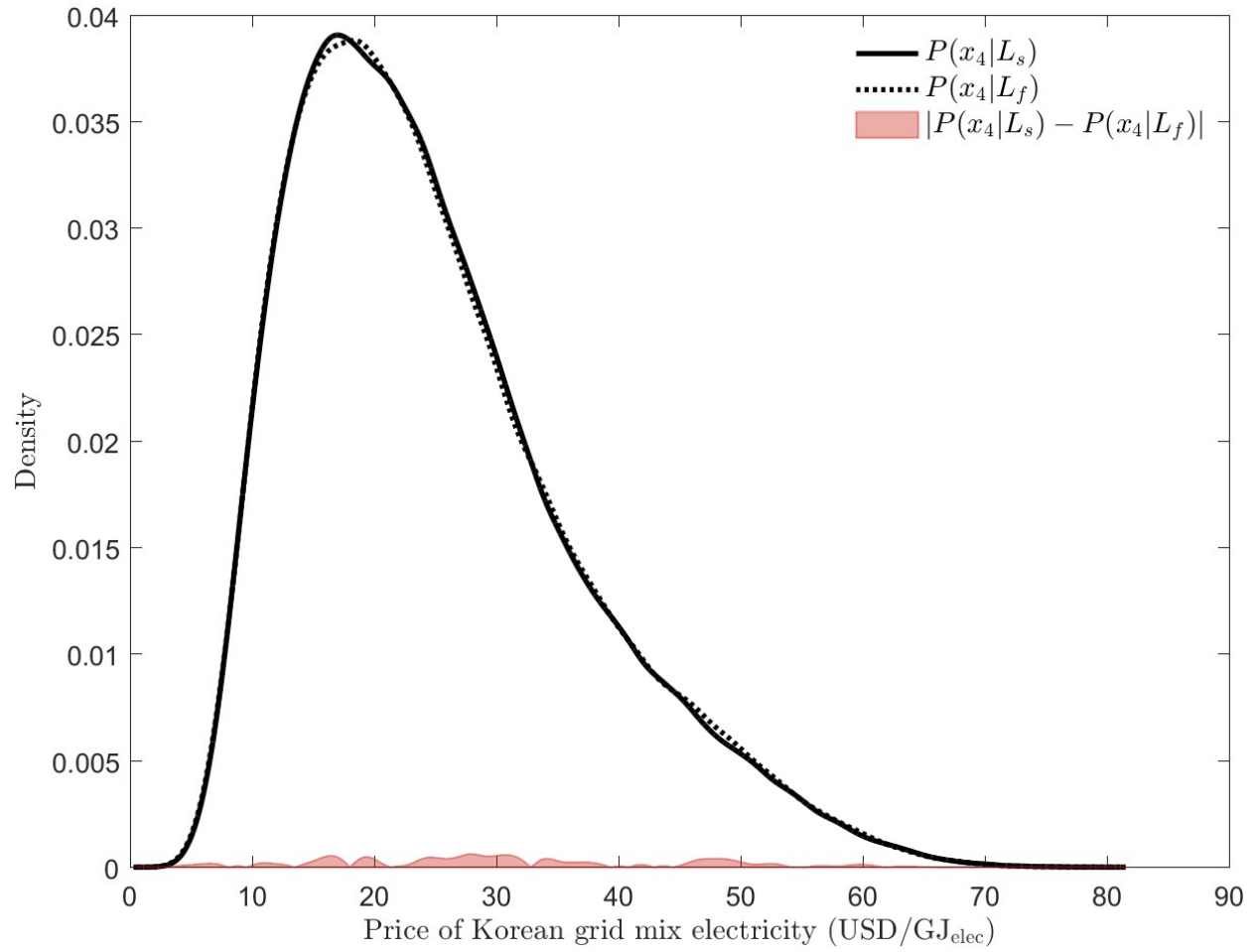


**Figure S23.** Likelihood distribution for Korean grid mix electricity price ( $x_4$ ), multi-criteria.

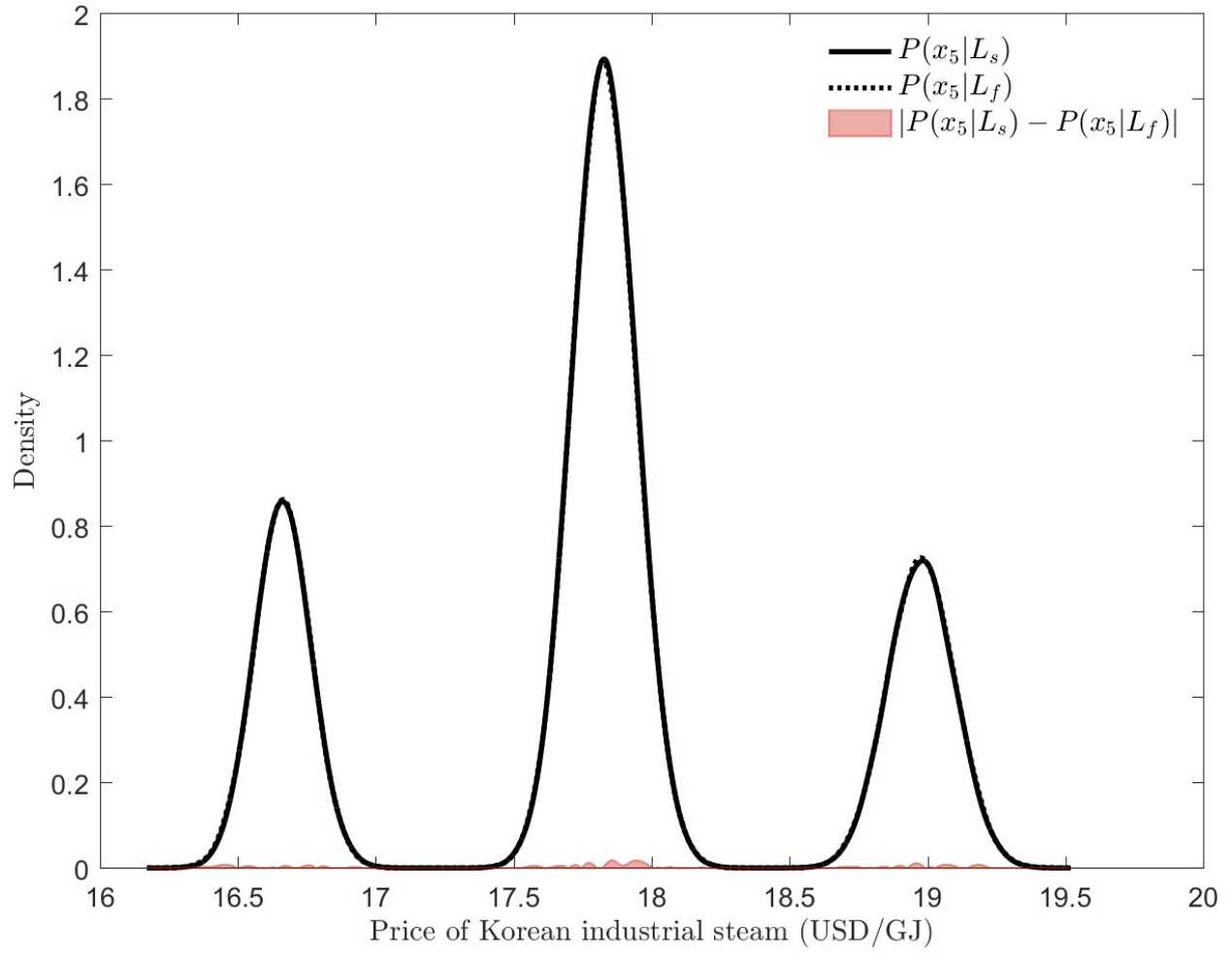


**Figure S24.** Likelihood distribution for Korean industrial steam price ( $x_5$ ), multi-criteria.

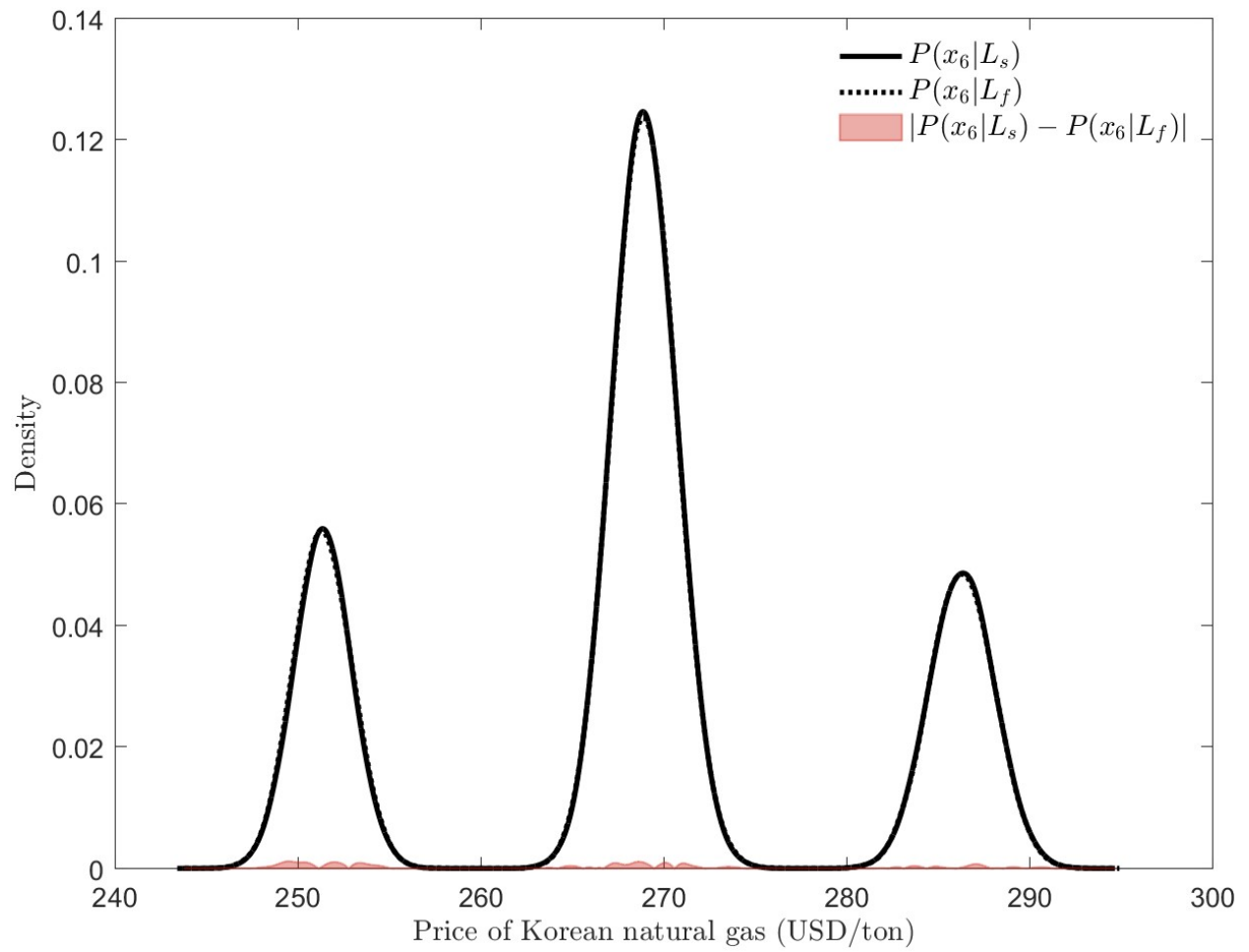


**Figure S25.** Likelihood distribution for Korean natural gas ( $x_6$ ), multi-criteria.

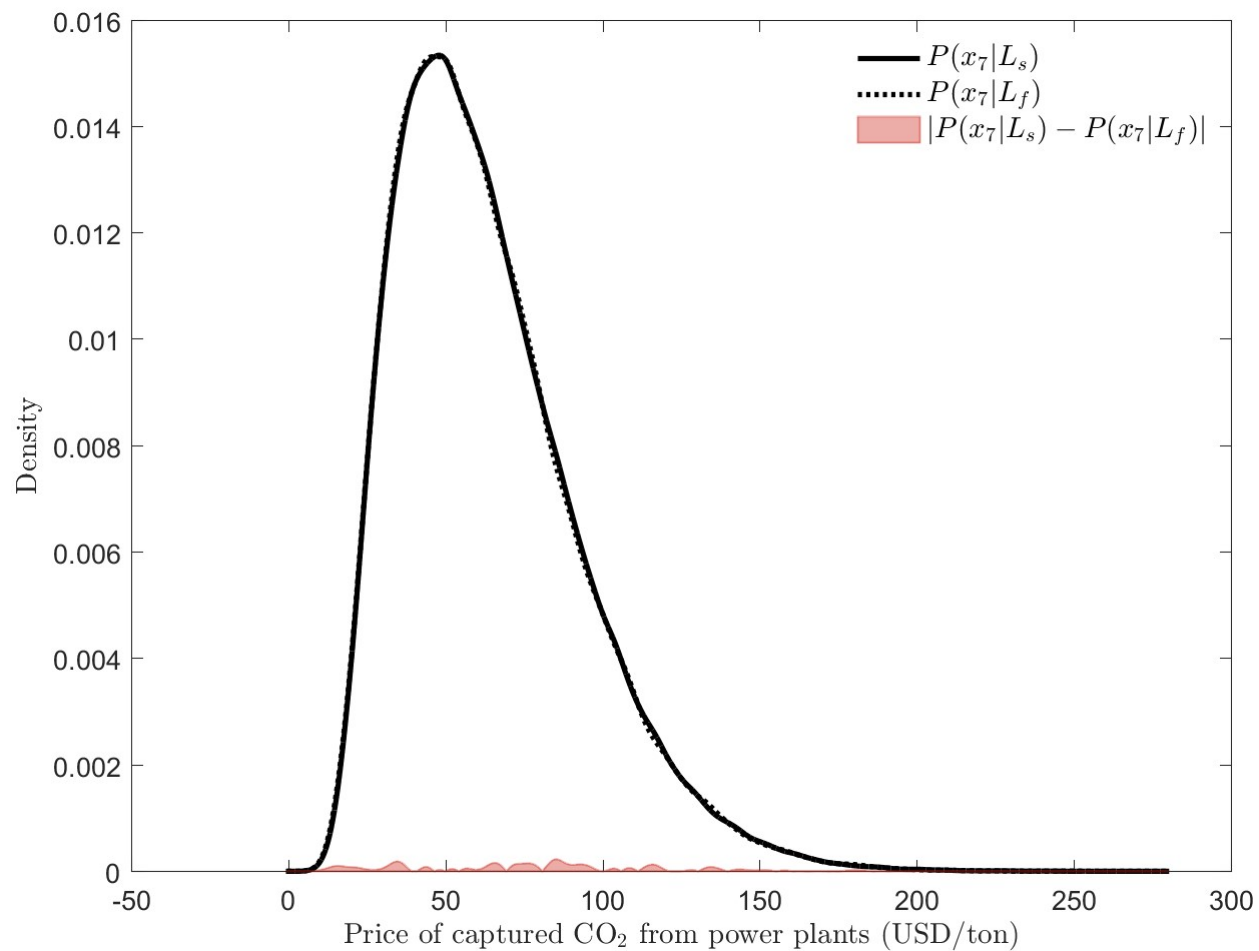


**Figure S26.** Likelihood distribution for the price of captured CO<sub>2</sub> from power plants ( $x_7$ ), multi-criteria.

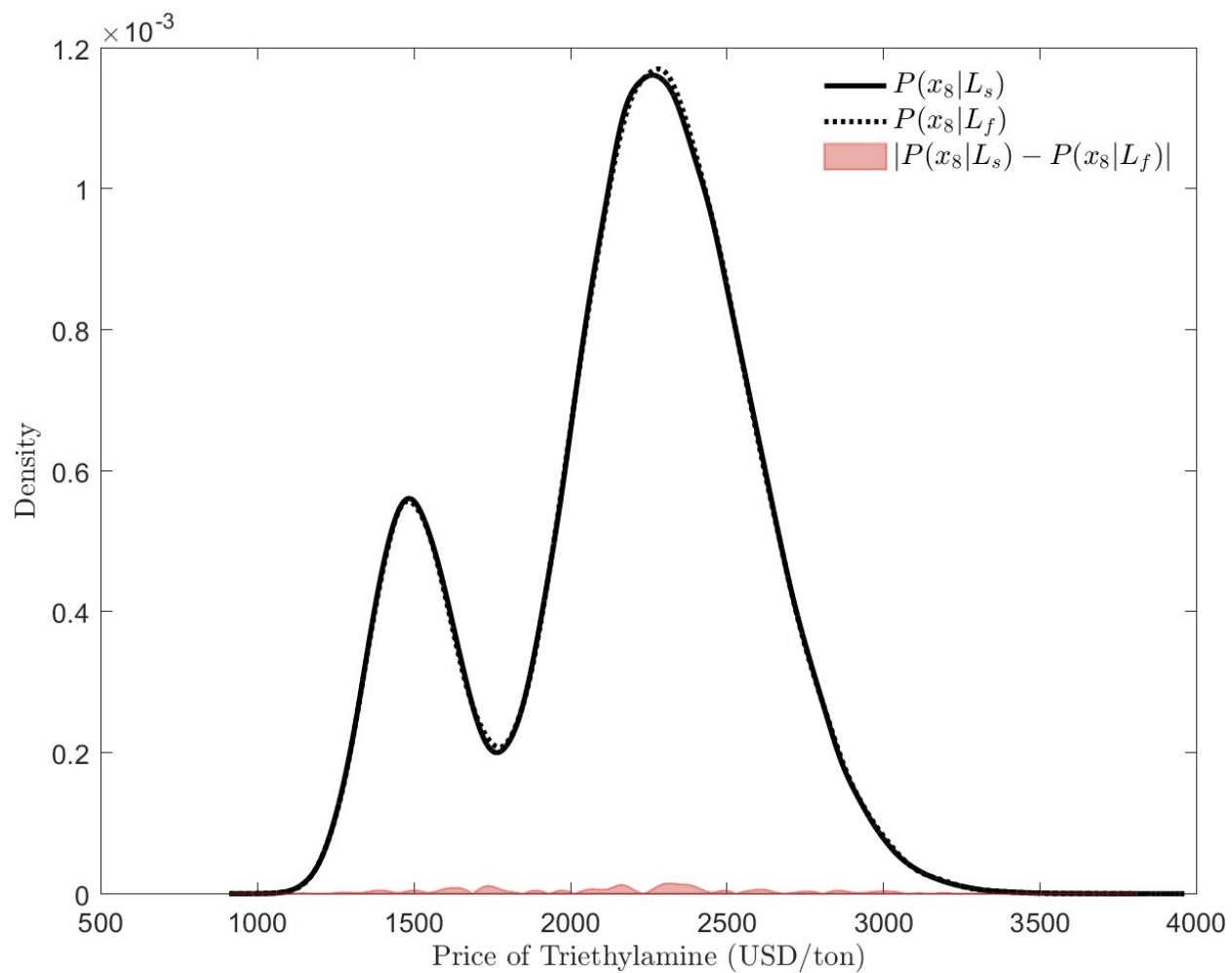


**Figure S27.** Likelihood distribution for the price of triethylamine ( $x_8$ ), multi-criteria.

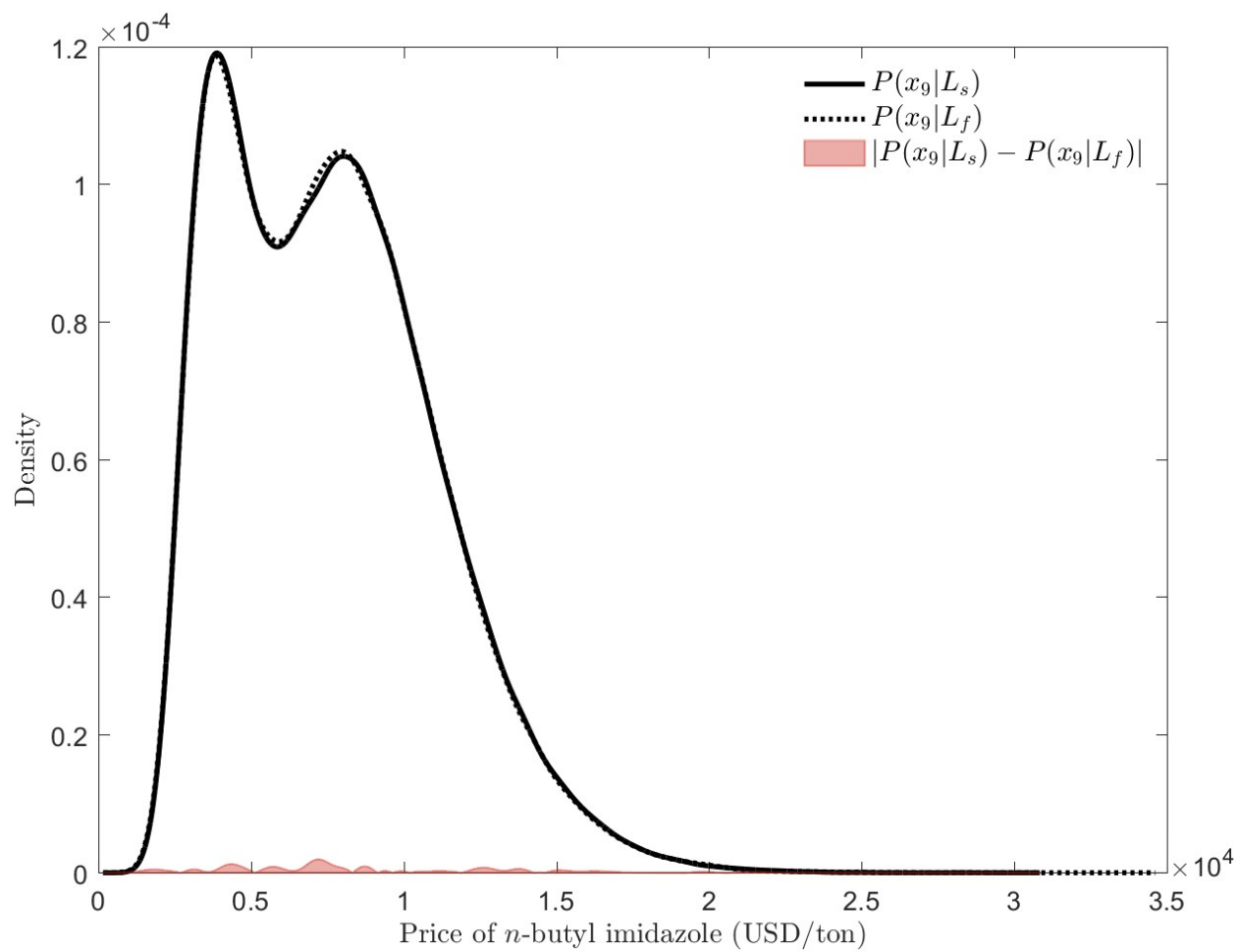


**Figure S28.** Likelihood distribution for the price of *n*-butyl imidazole ( $x_9$ ), multi-criteria

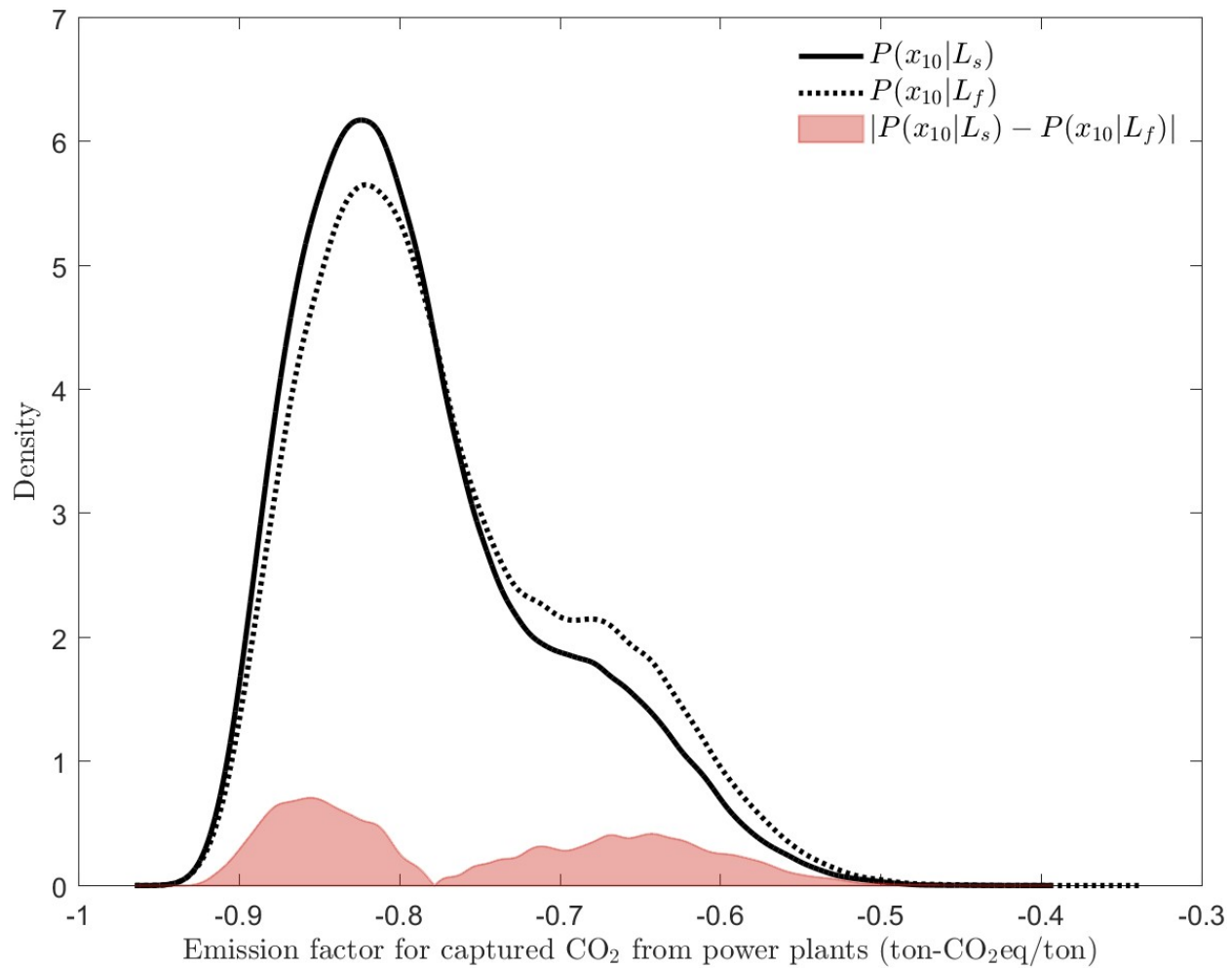


**Figure S29.** Likelihood distribution for the emission factor of captured CO<sub>2</sub> from power plants ( $x_{10}$ ), multi-criteria

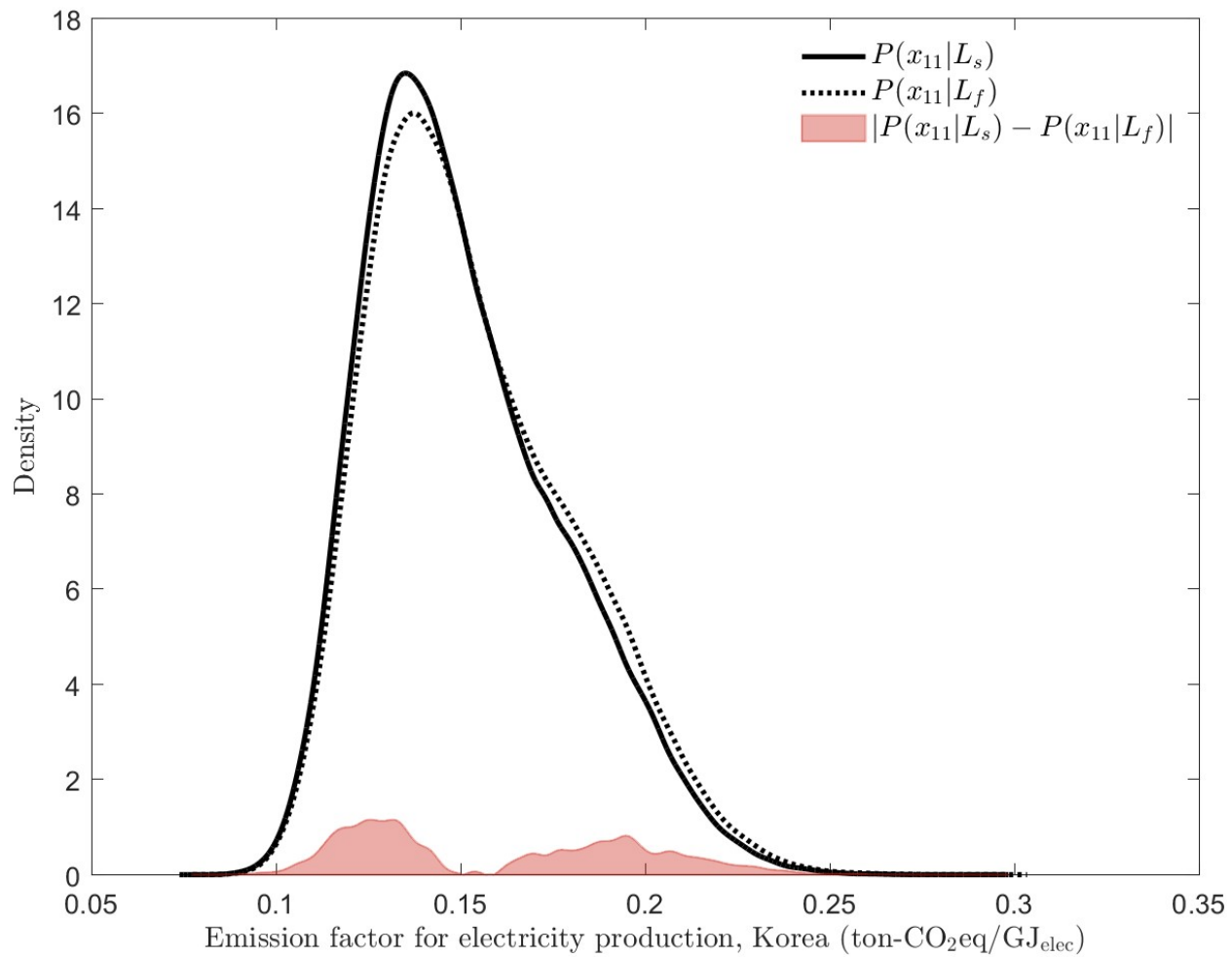


**Figure S30.** Likelihood distribution for the emission factor of Korean grid mix electricity production ( $x_{11}$ ), multi-criteria

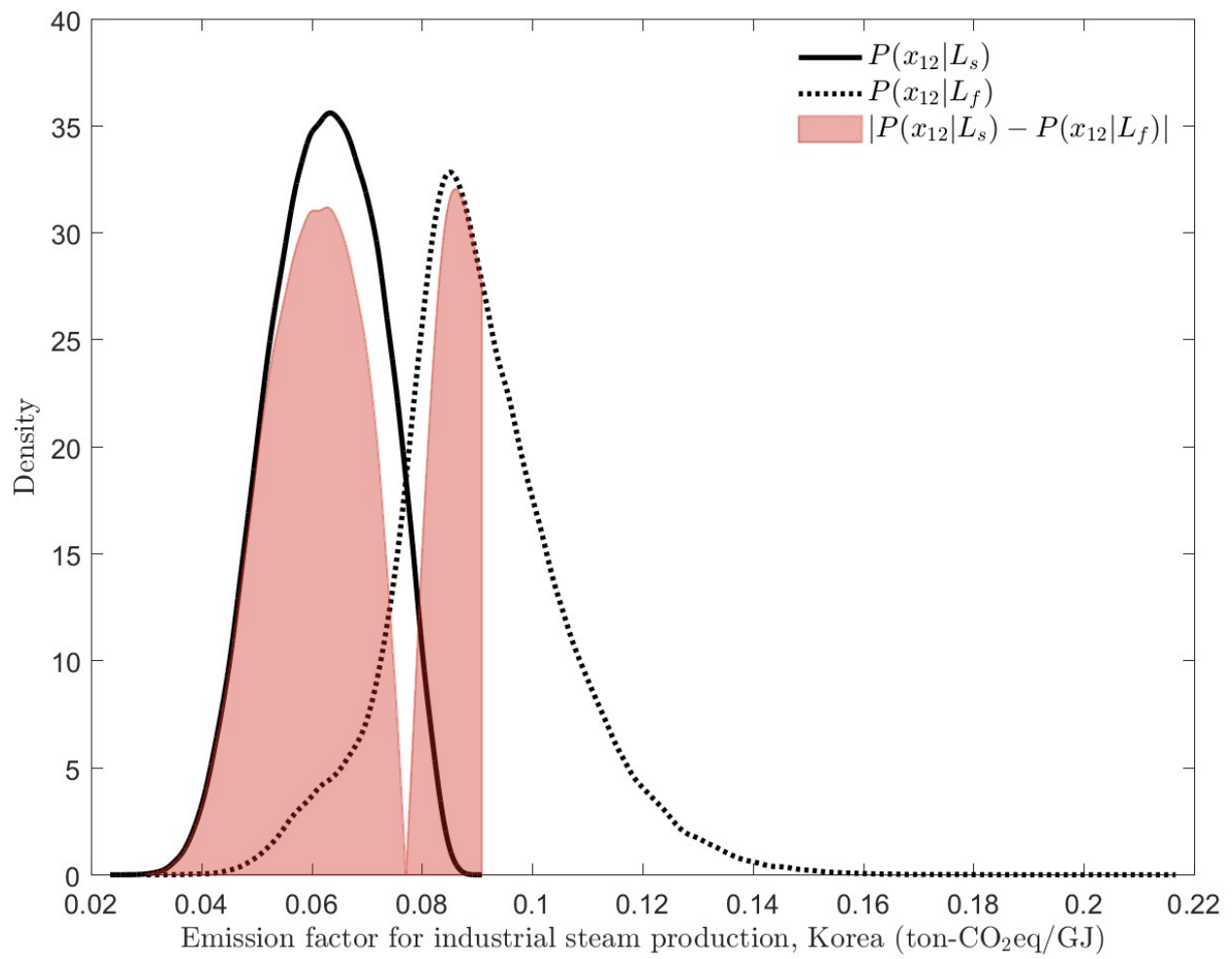


**Figure S31.** Likelihood distribution for the emission factor of Korean industrial steam production ( $x_{12}$ ), multi-criteria

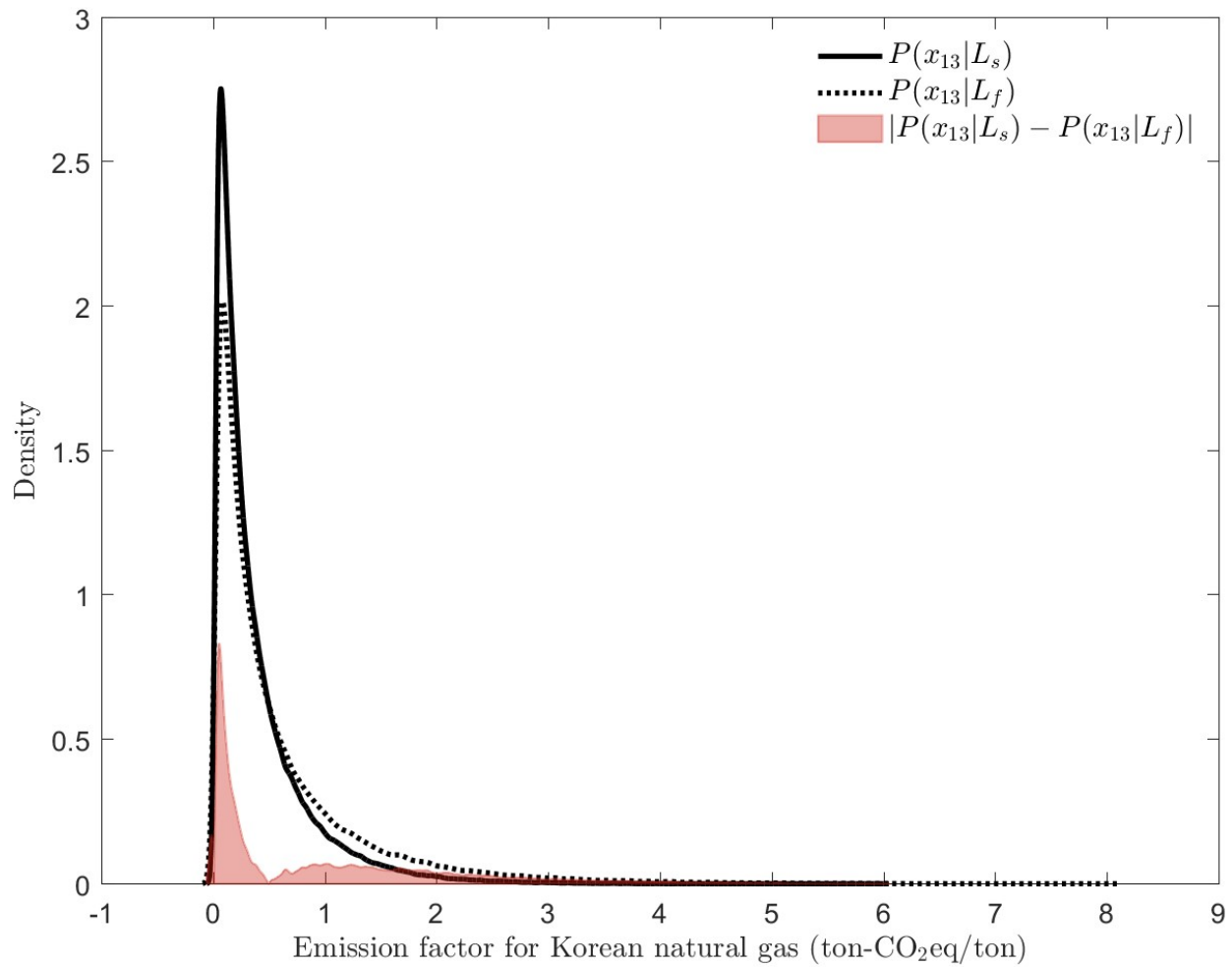


**Figure S32.** Likelihood distribution for the emission factor of Korean natural gas ( $x_{13}$ ), multi-criteria

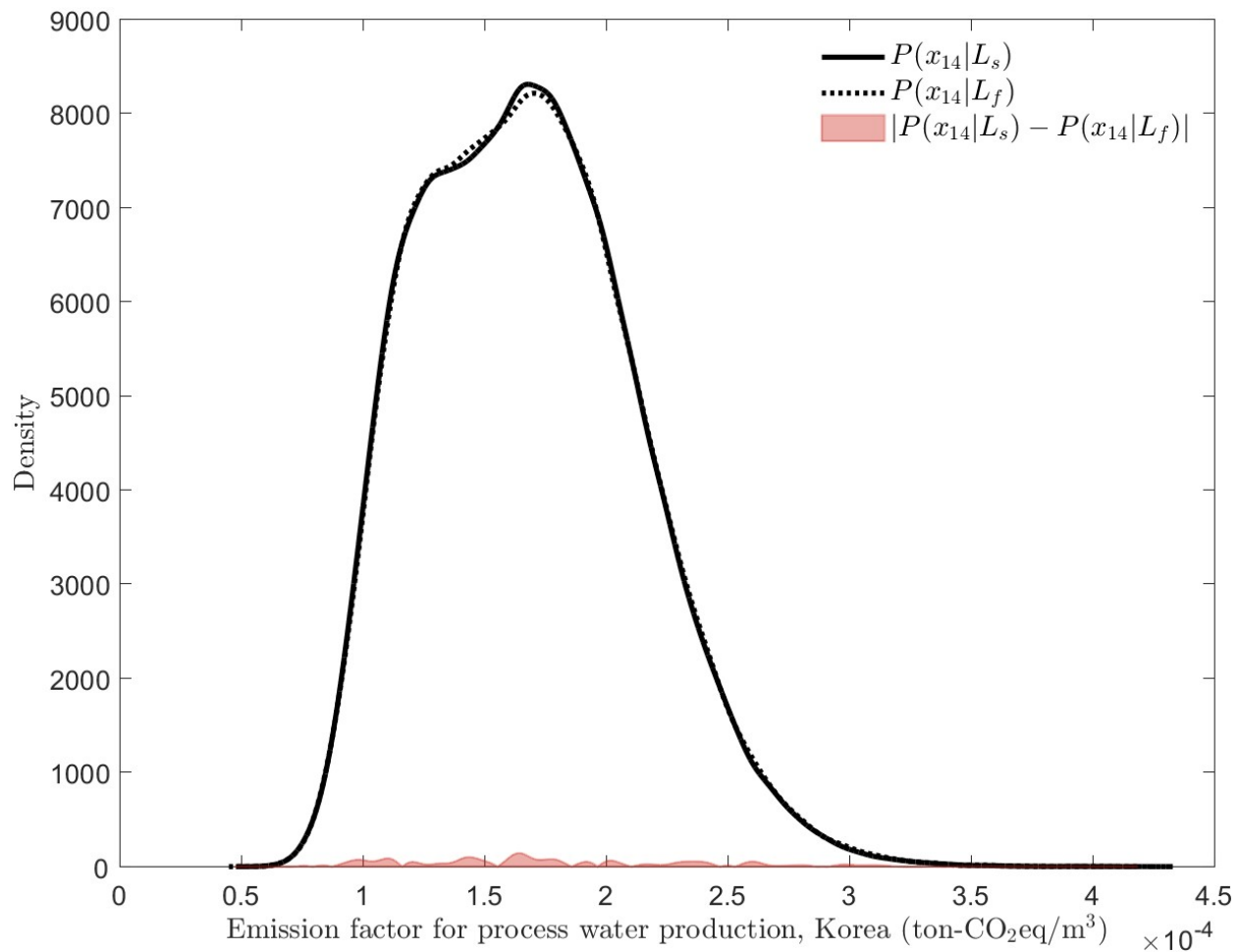


**Figure S33.** Likelihood distribution for the emission factor of Korean process water production and supply ( $x_{14}$ ), multi-criteria

## References

1. C. R. Stephens, H. F. Huerta and A. R. Linares, When is the Naive Bayes approximation not so naive?, *Machine Learning*, 2018, **107**, 397-441.
2. I. Rish, An Empirical Study of the Naïve Bayes Classifier, *IJCAI-01 Workshop on Empirical Methods in AI*, 2001.
3. P. Langley and S. Sage, presented in part at the Proceedings of the Tenth international conference on Uncertainty in artificial intelligence, Seattle, WA, 1994.
4. H. Zhang and C. X. Ling, A Fundamental Issue of Naive Bayes, *Canadian Conference on AI*, 2003, 591-595.
5. L. Tao, J. N. Markham, Z. Haq and M. J. Bidy, Techno-economic analysis for upgrading the biomass-derived ethanol-to-jet blendstocks, *Green Chemistry*, 2017, **19**, 1082-1101.
6. G. Towler and R. Sinnott, in *Chemical Engineering Design (Second Edition)*, eds. G. Towler and R. Sinnott, Butterworth-Heinemann, Boston, 2013, DOI: <https://doi.org/10.1016/B978-0-08-096659-5.00007-9>, pp. 307-354.
7. R. Davis, J. Markham, C. Kinchin, N. Grundle, E. C. D. Tan and D. Humbird, *Process Design and Economics for the Production of Algal Biomass: Algal Biomass Production in Open Pond Systems and Processing Through Dewatering for Downstream Conversion*, National Renewable Energy Laboratory (NREL), Golden, CO (United States), 2016.
8. G. Faber, C. Mangin and V. Sick, Life Cycle and Techno-Economic Assessment Templates for Emerging Carbon Management Technologies, *Frontiers in Sustainability*, 2021, **2**, 93.
9. K. Park, G. H. Gunasekar, S.-H. Kim, H. Park, S. Kim, K. Park, K.-D. Jung and S. Yoon, CO<sub>2</sub> hydrogenation to formic acid over heterogenized ruthenium catalysts using a fixed bed reactor with separation units, *Green Chemistry*, 2020, **22**, 1639-1649.

10. KEPCO, Electric Rates History,  
<https://cyber.kepco.co.kr/ckepco/front/jsp/CY/E/E/CYEEHP00375.jsp> (accessed 16 October 2021)).
11. CNCITY Energy, Rates for Heating,  
<https://www.cncityenergy.com/jsp/customer/chargeInfoHeat.jsp?menuId=883> (accessed 16 October 2021)).
12. Seoul City Gas, Rates for Heating and Natural Gas,  
<https://www.seoulgas.co.kr/front/payment/gasPayTable.do> (accessed 16 October 2021).
13. SK E&S, Heating Supply & Rates, <https://www.skens.com/gumi/rate/guide.do> (accessed 16 October 2021).
14. CNCITY Energy, Rates for City Natural Gas,  
<https://www.cncityenergy.com/jsp/customer/chargeInfoGas.jsp?menuId=827> (accessed 16 October 2021).
15. IEA, Levelised cost of CO<sub>2</sub> capture by sector and initial CO<sub>2</sub> concentration,  
<https://www.iea.org/data-and-statistics/charts/levelised-cost-of-co2-capture-by-sector-and-initial-co2-concentration-2019> (accessed 14 October 2021).
16. N. Thonemann and M. Pizzol, Consequential life cycle assessment of carbon capture and utilization technologies within the chemical industry, *Energy & Environmental Science*, 2019, **12**, 2253-2263.
17. R. M. Cuéllar-Franca and A. Azapagic, Carbon capture, storage and utilisation technologies: A critical analysis and comparison of their life cycle environmental impacts, *Journal of CO<sub>2</sub> Utilization*, 2015, **9**, 82-102.
18. I. Garcia-Herrero, R. M. Cuéllar-Franca, V. M. Enriquez-Gutiérrez, M. Alvarez-Guerra, A. Irabien and A. Azapagic, Environmental Assessment of Dimethyl Carbonate Production:

- Comparison of a Novel Electrosynthesis Route Utilizing CO<sub>2</sub> with a Commercial Oxidative Carbonylation Process, *ACS Sustainable Chemistry & Engineering*, 2016, **4**, 2088-2097.
19. N. von der Assen, P. Voll, M. Peters and A. Bardow, Life cycle assessment of CO<sub>2</sub> capture and utilization: a tutorial review, *Chemical Society Reviews*, 2014, **43**, 7982-7994.
  20. A. Sternberg and A. Bardow, Power-to-What? – Environmental assessment of energy storage systems, *Energy & Environmental Science*, 2015, **8**, 389-400.
  21. Korea Environmental Corporation, Local Life Cycle Inventory Formulation and Application Potential, <https://www.me.go.kr/home/file/readDownloadFile.do?fileId=158161&fileSeq=1> (accessed 18 October 2021)).
  22. J. H. Seo, H. J. Kim, S. H. Chung and K. H. Park, LCCO<sub>2</sub> analysis of wood-containing printing paper by mixed ratio of de-inked pulp and BTMP, *Journal of Korea TAPPI*, 2013, **45**, 46-55.